NUMERICAL SOLUTION OF HYDRODYNAMIC EQUATIONS FOR THE QUARK-GLUON PLASMA

by

HAFEEZ R. HOORANI

B.Sc.(Hons.), University of Karachi, 1980

M.Sc., University of Karachi, 1982

THESIS SUBMITTED IN PARTIAL FULFILLMENT OF

THE REQUIREMENTS FOR THE DEGREE OF

MASTER OF SCIENCE

in the Department

of

PHYSICS

SIMON FRASER UNIVERSITY

October 1986

APPROVAL

Name: HAFEEZ R. HOORANI

Degree: Master of Science

Title of thesis: NUMERICAL SOLUTION OF HYDRODYNAMIC EQUATIONS FOR THE QUARK-GLUON PLASMA

Examining Committee:

Chairman: Dr. R. Enns

Dr. D. H. Boal
Senior Supervisor

Dr. K. S. Viswanathan

Dr. M. Plischke

Dr. B. Jennings
External Examiner
TRIUMF

Date Approved: October 21st, 1986

PARTIAL COPYRIGHT LICENSE

I hereby grant to Simon Fraser University the right to lend my thesis, project or extended essay (the title of which is shown below) to users of the Simon Fraser University Library, and to make partial or single copies only for such users or in response to a request from the library of any other university, or other educational institution, on its own behalf or for one of its users. I further agree that permission for multiple copying of this work for scholarly purposes may be granted by me or the Dean of Graduate Studies. It is understood that copying or publication of this work for financial gain shall not be allowed without my written permission.

Title of Thesis/Project/Extended Essay

Numerical Solution of Hydrodynamic Equations for the Quark-Gluon Plasma

Author:

(signature)

H.R. HOORANI

(name)

NOV. 14, 1986

(date)

ABSTRACT

In this thesis the hydrodynamical expansion and the possible experimental signature of quark-gluon plasma formation in a heavy ion collision, are studied. Initial conditions are simulated by using the parton cascade picture to describe the collision of two heavy ions at relativistic energies. The hydrodynamical equations for the time evolution of the plasma are solved numerically using the two-step Lax-Wendroff method. The possible experimental signature considered here for the formation of quark-gluon plasma is the relative abundance of kaons to pions. This ratio is proportional to the ratio of the strange quark density to the entropy density up to the corrections due to the final state interactions. On the basis of simple models, it has been found that kaons to pions ratio is large and therefore, it has been proposed as the most promising signal for the formation of quark-gluon plasma. Using the computer simulation, (which includes finite size, realistic cross sections, full three dimensional treatment etc.) we find this ratio to be much smaller than the ratio obtained by other authors using simple models. We emphasize that it is not likely to be a useful signature for the formation of quark-gluon plasma.

ACKNOWLEDGMENTS

I would like to thank my supervisor David Boal first of all for giving me the problem to work on, and second for providing me the constant guidance and help during my work. Also I want to thank the members of the supervisory committee for their encouragement and answers to many of my questions. I also like to thank my roommate for his normal and abnormal behaviours. Finally, my special thanks to my friends Vikram Varma and Desiree Vanderwel for their constant encouragement and moral support.

DEDICATION

To my mother

TABLE OF CONTENTS

LIST OF FIGURES

CHAPTER 1

INTRODUCTION

During the past two decades, our concept of an elementary particle has undergone a fundamental change. All hadrons are now thought to be a composite state of more elementary entities known as quarks and gluons[1] Today it is known that there are at least five different flavours of quarks, called up(u), down(d), strange(s), charm(c) and bottom(b),respectively, and there are strong theoretical reasons to suspect the existence of one more flavour, called top(t). The quarks of various flavours differ widely by their mass. The quarks must carry one further internal quantum number which is called colour[2]. This can be deduced from the existence of particles,for example the $\Delta^{++}(1230)$, which contains three identical quarks with parallel spin in an s-wave state. The Pauli principle requires that the quarks differ from each other by an additional quantum number. There are three different colour degrees of freedom.The colour quantum number is exactly conserved and it acts as the source of a force field which is of long range unless screened. The theory which deals with colour forces is known as quantum chromodynamics(QCD). The binding force between quarks inside an hadron ,which is called the strong force, behaves quite differently than that associated with gravity or electromagnetism. Until now quarks have not been observed in isolation and the non-observation of an isolated quark implies that the force increases with separation. On the other hand, at high momenta or short distances , this force

becomes arbitrarily weak. For mediating the strong force between three different colour charges at least eight intermediate bosonic fields are needed; these fields are known as gluons. The predictions of QCD at large momenta or short distances are in good agreement with experiment. At large momenta QCD coupling becomes weaker and therefore, perturbation theory may give reliable results. This property of QCD is known as asymptotic freedom. This property of QCD and simple geometrical considerations imply the possibility of a very novel phase transition i.e. the transition from normal hadronic matter to a new form of matter known as the quark-gluon plasma. The possibility of such a phase transition can be illustrated with the help of following simple argument. The number density of normal nuclear matter is $\rho_0 \simeq 0.145 fm^{-3}$, i.e. only one nucleon per $7fm^3$, and the energy density is $E_N = m\rho_0 \simeq 0.15 GeV/fm^3$. On the other hand, the energy density within a typical hadron is $E_H \simeq 0.5 GeV/fm^3$ which is three times the energy density of normal nuclear matter. Thus, with a modest increase of energy density from E_N to E_H, the dilute conditions will change to a dense condition in which neighboring hadronic wave functions overlap and the internal degrees of freedom, which are associated with quarks and gluons, become activated. This increase in energy density can be achieved either by compressing cold nuclear matter or heating up the matter and filling the space between the nucleons with mesons. This implies that at even higher energies normal hadronic matter will possibly go through a phase transition. The value of the temperature at which this

transition occurs is not well established, but different theoretical speculations[3-5] and the lattice Monte Carlo simulations[6-8] give a value of the order of 150-300MeV. Matter has already gone through such a phase transition in the very early universe when very high temperatures and pressures existed. Under laboratory conditions, it may be possible to create the quark-gluon plasma in the head on collision of two heavy nuclei (A=197 to 238) at ultrarelativistic energies (E=10 to 100GeV/A).At ultrarelativistic energies and with zero impact parameter nuclei are sufficiently transparent to nucleons that in a central collision the nuclei pass through each other, producing two highly excited nuclear fragmentation regions containing the net baryon number of the system. One of these regions is known as the target fragmentation region(TFR) corresponding to the target and other is known as the beam fragmentation region(BFR) corresponding to the projectile. As in NN collisions[9] these are expected to be joined together by a central rapidity region (CRR) with small net baryon number. The nuclear transparency just mentioned above is a result of strong time dilatation and Lorentz contraction. To understand nuclear transparency, consider a central collision of two nuclei with A >> 1 which are moving with an equal and opposite velocity v relative to the centre of mass. The velocity is such that the Lorentz factor $\gamma >> 1$. In the longitudinal direction the nuclei are Lorentz contracted to a length $2R_A/\gamma \simeq 2A^{1/3}/\gamma$ where R_A is the radius of the nucleus. A basic ingredient in the space-time description of the collision is the existence of a strong

interaction proper time scale $\tau_0 = 1/\Lambda_{qcd} \simeq 1$fm/c. In any hadronic collision, the produced fragments can only reinteract after a proper time τ_0 has elapsed after their production. If one now increases γ ,the nuclei finally are so much Lorentz contracted that they entirely cross each other in a time less than τ_0. The laboratory conditions and the condition which existed in the very early universe for the plasma are the same except for one major difference: the rate of cooling of the plasma. In case of the early universe the cooling was slow (of the order 10^{-6}sec), whereas in the laboratory the rate of cooling is very fast (of the order 10^{-23}sec). In chapter 2 of this thesis nuclear transparency is discussed in detail.

To create and study such a primordial plasma in the laboratory is one of the challenges for present day theoretical and experimental physics. The indications that such a novel form of matter can exist raises many difficult questions. First of all during the formation of the quark-gluon plasma, hadronic matter goes through the deconfinement phase transition and one would like to study the nature of this phase transition. The study of phase transitions requires the complete understanding of the statistical behaviour of the system which is equivalent to determining the grand canonical partition function of the system. For finding the grand canonical partition function one needs to know the exact form of the Hamiltonian of the system. To know the Hamiltonian, one needs an understanding of the interactions between the different constituents of the system.

In our case it is equivalent to requiring comprehensive understanding of QCD, which is at present far from being completely understood.

Another question is how much time does the system spend as a quark-gluon plasma, how much time as a mixed phase and how much time as hadronic matter before the matter decouples? How does this depend upon the initial conditions and the baryon number of the colliding nuclei? To study this question we need to know the time evolution of the plasma. The time evolution of the plasma has been studied in the recent past[10,11] with special emphasis on the central rapidity region. There have been two reasons for this: first, this region shows approximately a plateau structure for the particle production as a function of the rapidity variable in pp collisions at very high energies, thus implying boost invariance along the collision axis; second, the net baryon number is close to zero and thus one can work with zero chemical potential. It has, however, been known since the beginning that these two simplifications do not apply to the reaction conditions achievable in the experiments planned in near future[12]. It is also known that the stopping power[13,14] of nuclei is larger than what it was believed to be just a few years ago, therefore, the net baryon number will not necessarily be small. The time evolution of the plasma and nuclear stopping power will be discussed in chapter 2. The expansion dynamics of the plasma can still be studied easily if one makes the assumption of local thermal equilibrium. In this case the plasma

can be treated as a hydrodynamically expanding fluid and one can apply the laws of relativistic hydrodynamics. Hydrodynamics has a long history as a means of treating collisions of strongly interacting systems. It's application was originally proposed by Landau[15] in 1953, and it has been used to discuss very high energy pp collisions.[16-19] The application of hydrodynamics to the reaction of heavy nuclei seems more plausible than for pp collisions. Here the system is so large relative to the mean free path that the assumption of the local thermal equilibrium is not unjustified and so too the use of hydrodynamics.

The equations which describe the hydrodynamic evolution of the plasma depend only on the condition of matter at some fixed time, and upon the equation of state which relates energy density and pressure. The boundary conditions may be chosen either as initial conditions or as the final configuration at very late times when the matter freezes out and subsequently evolves as free streaming particles to detectors. To determine the equation of state is equivalent to finding out the velocity of sound in the quark-gluon plasma. Recently Gavai and Gocksch[20] tried to determine the velocity of sound using a lattice Monte Carlo calculation. In this work, an equation of state with all of the properties needed to describe the change from an ideal hadronic gas (a description valid at low temperatures) to an ideal quark-gluon plasma (valid for high temperatures),[21-23] is provided by the MIT bag model.

The thermodynamics of the plasma will be discussed in chapter 2. There the partition function and other thermodynamic variables are calculated in the hadronic phase without the assumption of massless particles. Also a brief review of the MIT bag model is given in chapter 2. Hydrodynamics of the plasma is discussed in detail in chapter 2 as well. All the dissipative effects such as viscosity and thermal conductivity in the plasma will be neglected and only the relativistic ideal hydrodymanics will be discussed. For treating the plasma expansion exactly i.e. including the dissipative effects we need to know the full QCD kinetic theory and at present we do not know how to correctly treat A+A collisions in the QCD kinetic theory.

One of the very important questions is the experimental signature of the plasma formation. All the characteristic kinematical signatures of the plasma formation would almost with certainty be destroyed by the hadronic final state interactions. An exceptional case may be the scenario [24,25] of massive supercooling of the plasma phase during the expansion. There the subsequent transition to the hadronic phase proceeds like an explosion producing shock waves that should be clearly visible in the transverse momentum distribution of the emitted hadrons.

Any analysis promising success must be based on the observation of properties that are not affected by final state interactions. Two such observables are:

(a) particles that do not interact strongly (production of dileptons), [26-28] and

(b) quantum numbers that remain unchanged by strong interactions (strangeness production).[29,30]

Most of the work in this thesis related to the possible experimental signatures for the plasma formation is concentrated on strangeness production. The significant changes in relative and absolute abundance of strange particles such as Λ could serve as a possible probe for quark-gluon plasma formation.[31] Different strangeness producing mechanisms and the relevant production rates as functions of the energy density of the plasma state have been studied by Rafelski and Muller.[30] Another possibility concerning strangeness production as a signal for plasma formation is studied recently by J. Kapusta.[32] In his work he has studied K^-/π^- ratio as a possible signature for the plasma formation. The production of dileptons and strangeness as possible experimental signatures are discussed in detail in chapter 4.

The overall organisation of this thesis is as follows: In chapter 2 the time evolution, thermodynamics, hydrodynamics, equation of state and the bag model of the plasma are discussed. In chapter 3 the numerical solution of the hydrodynamic equations using an appropriate finite difference scheme is discussed. This discussion will also include the initialization and the stability analysis of the numerical solution. In chapter 4 the most promising experimental signatures of the plasma formation are discussed. We will mainly concentrate on the strangeness production . Chapter 5 contains the conclusion and

suggestions for the further research.

CHAPTER 2

THERMODYNAMICS AND HYDRODYNAMICS OF QCD PLASMA

This chapter will start with a brief review of the thermodynamics of the quark-gluon plasma. The motivation for such a review is as follows: first of all, the knowledge of different thermodynamical variables and relations of both phases will be helpful in motivating the phase transition from the hadronic phase to the quark-gluon plasma phase. Secondly, using a simple model, which will be outlined in the next section, one can get rough estimates of the transition temperature and the latent heat of the transition. In discussing the thermodynamics of quark-gluon plasma phase, attention will be focused on the baryon symmetric plasma (i.e. the chemical potential μ_p=0). The hadronic phase will be assumed to be a gas of massless pions. Obviously, the above assumptions are oversimplified but still this model roughly describes the picture of the phase transition. In the next section, a summary of the results obtained from lattice QCD are also quoted. This chapter will include ideal relativistic hydrodynamics of the quark-gluon plasma. It will also include a discussion of the Bjorken-type picture of the time evolution of the plasma.

2.1 THERMODYNAMICS OF HADRONS AND PLASMA:

The grand partition function for a many particle system at temperature T and chemical potential μ is defined as[33]

$$Z = Tr\ [\exp\{-(H - \mu N)/T\}] \ . \qquad (2.1)$$

Here Boltzmann's constant is taken to be one and for later discussion it is assumed that both Planck's constant and velocity of light are equal to unity. In the above equation H is the Hamiltonian of the system and N is the particle number operator. All the formulas given below are valid for single component systems and the generalization of the treatment to several kinds of particles is straightforward. In the grand canonical ensemble both the energy and particle number fluctuate and their average values can be obtained in terms of Z as

$$\epsilon = E/V = (1/V)\ Tr[H \exp\{-(H - \mu N)/T\}]/Z$$
$$= (T^2/V)\ \partial \ln Z/\partial T + \mu n, \qquad (2.2)$$

$$n = N/V = (1/V)\ Tr[N \exp\{-(H - \mu N)/T\}]/Z$$
$$= (T/V)\ \partial \ln Z/\partial \mu \ . \qquad (2.3)$$

The logarithm of the grand partition function of particles and antiparticles with mass m, chemical potential μ and degeneracy factor g in the large volume limit of a free gas is:

$$\ln Z = gV(6\pi^2T)^{-1}\int_0^\infty dk\, k^4 (k^2+m^2)^{-1/2}\{[\exp\{[(k^2+m^2)^{1/2} - \mu]/T\}+\eta]^{-1} + [\exp\{[(k^2+m^2)^{1/2}+\mu\,]/T\}+\eta]^{-1}\} \quad (2.4)$$

with $\eta = 1$ for fermions and $\eta = -1$ for bosons. In order to calculate the entropy density s and pressure P first recall the first law of thermodynamics

$$dE = T\,dS - P\,dV + \mu\,dN \quad (2.5)$$

which implies that the energy E is a thermodynamic function of the total entropy S, the volume V and the number of particles N. But for a grand canonical ensemble N is a varying quantity and therefore, another set of variables is more convenient than (S,V,N). One possible choice is (T,V,μ) and the change of variables can be obtained by using a Legendre transformation i.e.

$$\Omega\,(T,V,\mu) = E - TS - \mu\,N \quad (2.6)$$

where Ω is the thermodynamic potential. The differential of equation (2.6) with the use of (2.5) leads to the following relation

$$d\Omega = -S\,dT - P\,dV - N\,d\mu \quad (2.7)$$

where

$$S = -(\partial\,\Omega/\partial\,T),\ P = -(\partial\,\Omega/\partial\,V),\ N = (\partial\,\Omega\,/\partial\,\mu)\ . \quad (2.8)$$

The thermodynamic potential is also related to the grand partition function through the following relation

$$\Omega\ (T,V,\mu) = -\ T\ \ln Z\ . \tag{2.9}$$

Equation (2.8) and (2.9) together give

$$s = (1/V)\partial(T\ \ln Z)/\partial T, \tag{2.10}$$

$$P = \partial(T\ \ln Z)/\partial V = -\ \Omega/V. \tag{2.11}$$

Also by putting (2.11) in (2.6)

$$\epsilon = -P + s\ T + \mu\ n\ . \tag{2.12}$$

In the case of fixed volume

$$dP = s\ dT + n\ d\mu; \tag{2.13}$$

$$d\epsilon = T\ ds + \mu\ dn\ . \tag{2.14}$$

If there is no constraint on the particle number, the equilibrium value of N corresponds to a vanishing chemical potential. Then (2.12), (2.13) and (2.14) reduce to

$$\epsilon + P = Ts;\ dP = s\ dT;\ d\epsilon = T\ ds;\ \mu = 0. \tag{2.15}$$

The momentum integral in equation (2.4) can be calculated exactly both for fermions and bosons if they are assumed to be

massless

$$T\ln Z_q = g_q (V/12)[(7/30)\pi^2 T^4 + \mu_q{}^2 T^2 + 1/(2\pi^2)\mu_q{}^4] \qquad (2.16)$$

$$T\ln Z_g = (g_g V/90)\pi^2 T^4 \ . \qquad (2.17)$$

For a free gas of quarks with two flavours and gluons, one finds the grand partition function of quarks, antiquarks and gluons

$$T\ln Z = [(37/90\pi^2)T^4 + \mu_q{}^2 T^2 + 1/(2\pi^2)\mu_q{}^4]V \qquad (2.18)$$

where the degeneracy factors in accordance with the SU(3) gauge structure of QCD are calculated as

$$g_q = 2 \times 2 \times 3 = 12 \ , \ g_g = 2 \times 8 = 16$$

For a pion gas the degeneracy factor is three and therefore, from (2.17)

$$T \ln Z_\pi \simeq (V/30)\pi^2 T^4 \qquad (2.19)$$

at the temperature $T >> m_\pi$. Finally, an extra term is introduced in the partition function for the quark-gluon plasma which modifies eqn. (2.18) as follows:

$$T\ln Z_p = [(37/90)\pi^2 T^4 + \mu_q{}^2 T^2 + 1/(2\pi^2)\mu_q{}^4 - B]V. \qquad (2.20)$$

This extra term contains the bag constant B, which takes into

account the difference of energy of true and QCD vacuum ground states[34]. As it was mentioned earlier that the plasma phase is taken to be baryon symmetric i.e. $\mu_q=0$, one gets from eqn. (2.20)

$$T\ln Z_p=[(37/90)\pi^2T^4-B]V. \tag{2.21}$$

The energy density and pressure in the plasma phase can be obtained by using eqn's (2.2), (2.11) and (2.21)

$$\epsilon_p= (37/30)\pi^2T^4+B, \tag{2.22}$$

$$P_p= (37/90)\pi^2T^4-B. \tag{2.23}$$

For the gas of massless pions, one can obtain the following relations for the energy density and pressure by using eqn's (2.19), (2.2) and (2.11),

$$\epsilon_h=(1/10)\pi^2T^4, \tag{2.24}$$

$$P_h=(1/3)\epsilon_h= (1/30)\pi^2T^4. \tag{2.25}$$

2.1.1 PHASE TRANSITION:

Now all the thermodynamic variables are known for both phases and one can construct a first order phase transition by using the Gibbs criteria i.e.

$$T_p=T_h=T_c \ ; P_p=P_h=P_c \ , \tag{2.26}$$

where p, h and c refer to the plasma phase, hadronic phase and transition region respectively. In constructing the first order phase transition one should remember the following

(a) only those solutions of equation (2.26) are acceptable which correspond to a stable hadronic phase at low densities,

(b) the latent heat, $\epsilon_1 - \epsilon_2$ must be non-negative.

The transition temperature T_c for a first order phase transition is determined by the condition:

$$P_h(T_c) = P_p(T_c)$$

to be

$$B = (34\pi^2/90)\, T_c^4$$

For B = 318MeV/fm^3 ,the transition temperature is [32]

$$T_c = 160\text{MeV}$$

The energy density corresponding to T_c and the latent heat of the transition are

$$\epsilon = 1.31\text{GeV/fm}^3$$

$$\Delta\epsilon = 1.23\text{GeV/fm}^3$$

Therefore, using this simple model a rough estimate of transition temperature is found.

2.1.2 RESULTS OF LATTICE GAUGE THEORY:

The idea of the phase transition from hadronic matter to the quark-gluon plasma is also supported by the results of lattice gauge theory. This is a numerical non-perturbative approach to finite temperature QCD,[35,36] which allows one to treat the interaction exactly. This scheme is based on a stochastic sampling of the exact functional integral for the partition function of finite temperature QCD defined on a space-time grid.

The partition function for a system described in terms of fields A(x) by a Hamiltonian H[A] is

$$Z = \mathrm{Tr}[\exp(-\beta H[A])], \tag{2.27}$$

where $1/\beta$ is the temperature. The formulation of the theory for pure SU(3) Yang-Mills theory can be described in three steps.
(a)The partition function Z is rewritten in the form of a functional integral over Euclidian space-time (i.e. with imaginary time variable):

$$Z(\beta,V) = \int (DA)\exp[\int d\tau \int d^3x L(A)], \tag{2.28}$$

where L(A) is the Lagrangian of the Yang-Mills field:

$$L[A] = -(1/4)(\partial_\mu A^a_\nu - \partial_\nu A^a_\mu + g f_{abc} A^b_\mu A^c_\nu)^2. \tag{2.29}$$

The integration runs over all field configurations.
(b)In the next step, the Euclidian x-τ continuum is replaced by

a finite lattice, with N_x sites of spacing a_x in the three spatial directions, and N_τ sites of spacing a_τ in the time direction.

(c)In the last step, the gauge field variable $A[(1/2)(x_i+x_j)]$ associated with the link between two adjacent lattice sites i and j is replaced by the gauge transformation

$$U_{ij}=\exp[-(i/2)\lambda_a(x_i x_j{}^{\mu}A^a_{\mu}]. \qquad (2.30)$$

In this way the integration over all field configurations is transformed into an integration over all elements of colour SU(3) at each lattice link. This gives us the partition function of the system and using that one can easily get the expression for the energy density.

Figure (1) shows a plot of the ratio ϵ/ϵ_{SB} versus T/Λ_L for a lattice of size 10x10x10x4.[35] Here ϵ_{SB} refers to the energy density obtained by using the Stefan-Boltzmann law for an ideal gas of gluons, Λ_L is the lattice parameter which has a typical value of 2MeV. The Fig. (1) shows a sudden drop of ϵ/ϵ_{SB} from one to zero when the temperature T falls below about $80\Lambda_L$, corresponding to a value of the critical temperature T_c= 208±20MeV. The above results are obtained for pure gluonic matter. This is shown instead of a gas of quarks and gluons because of the problems which from inclusion of fermions on the lattice.[36]

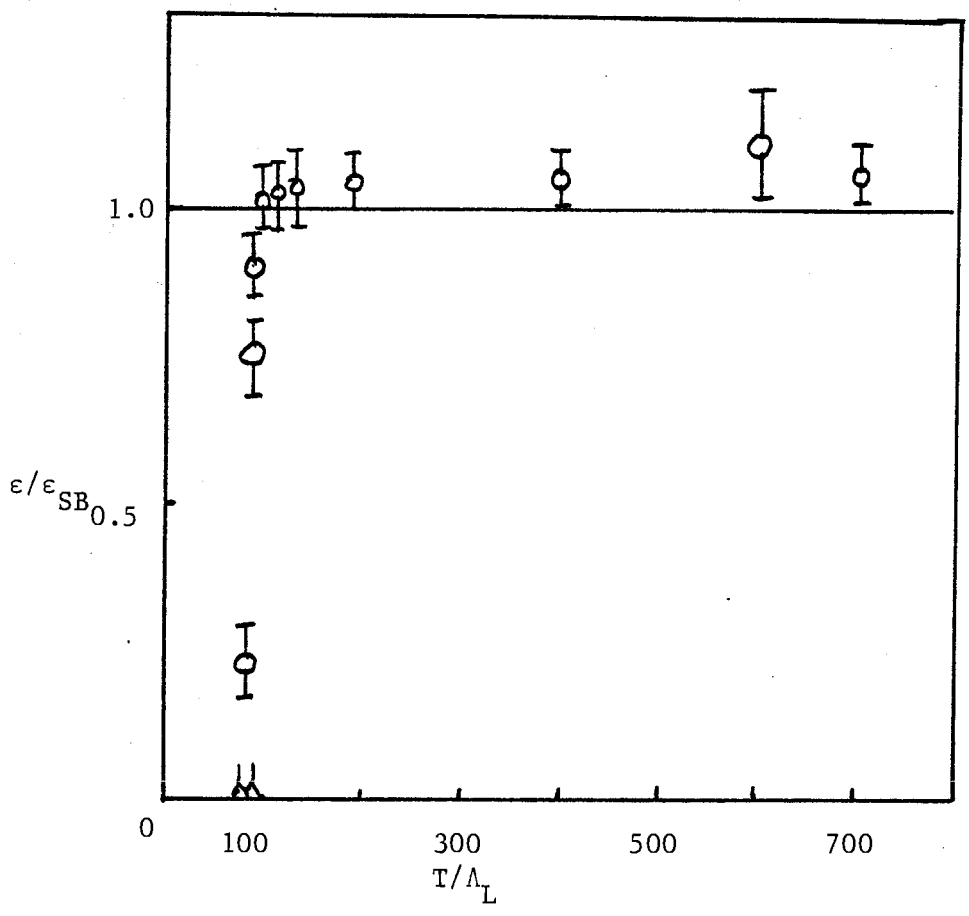

Fig. 1. The Monte Carlo simulation of pure SU(3) gauge theory.

The conclusions of above discussion can be summarized as follows: the deconfinement phase transition seems to be a first order phase transition. The simple thermodynamical model used here and the more involved calculations of lattice QCD leads to a temperature range for the transition between 150MeV and 250MeV. In case of lattice QCD calculations, what the result will be for the full theory inculding quarks is under heavy dispute and must be decided by future calculations.

2.2 HYDRODYNAMICS OF QUARK-GLUON PLASMA:

The validity of the hydrodynamical description is dependent upon the very important assumption that there is local thermal equilibrium. To decide whether or not the plasma is in local thermal equilibrium very much depends upon the initial conditions and time evolution of the plasma. Consider a central collision of two heavy ions with equal numbers of nucleons, A, at ultrarelativistic energies. At ultrarelativistic energies nuclei are highly Lorentz contracted in the direction of motion and sufficiently transparent to nucleons. The nuclear transparency is a result of time dilation ,length contraction and the uncertainty principle.[14] The idea can be illustrated as follows: A basic ingredient in the space-time description of the collision where particles are interacting through the strong interaction is the existence of a strong interaction proper time scale[37]

$$\tau_0 \simeq 1/\Lambda_{qcd} \simeq 1 fm/c$$

In any hadronic collision, the produced fragments can only reinteract after a proper time τ_0 has elapsed after their production. The rapidity variable is

$$y = 1/2 \ln[(1+v)/(1-v)] \qquad v=p/E$$

$$v = z/t = \tanh y, \quad z = \tau \sinh y, \quad t = \tau \cosh y$$

At the moment of collision, the system is excited to a state containing virtual fragments which materialize after a proper time τ_0 = 1fm/c has elapsed.[37] The virtual particles which are moving with a rapidity y materialize after travelling a distance

$$l(y) = vt = \gamma v \tau_0$$

$$\tau_0 \sinh y \simeq \exp(y) \tau_0/2 . \qquad y>>1$$

The l(y), which is known as the formation length[3,14] increases exponentially with the rapidity variable. This exponential growth of length scales is also referred to as longitudinal growth. On the other hand the formation time of a particle increases linearly with the energy of that particle; that is,

$$t = \gamma\tau_0 = (E/M)\tau_0$$

Also, nuclei are moving with a velocity which is close to velocity of light. Therefore, they are highly Lorentz contracted to a length $2R_A/\gamma$ (where R_A is the nuclear radius) in the direction of motion. In brief, an increase in the energy of a

nucleus increases the formation length of virtual fragments i.e. secondary particles and decreases the length of a nucleus in the direction of motion. Therefore, at very high energies a nucleon can pass through a nucleus with little interaction and this is the origin of nuclear transparancy.

In a central collision the nuclei pass through each other, producing two highly excited nuclear fragmentation regions containing the net baryon number of the system and these are joined together by a central rapidity region with small net baryon number but substantial energy density.[11] The post collision geometry in the centre of mass frame, in which the nuclei are both highly Lorentz contracted pancakes, is represented in Fig. 2. The time evolution of the central rapidity region has been studied by Bjorken[11] with the assumption that at sufficiently high energy there is a central plateau structure for the particle production as a function of the rapidity variable. The essence of this assumption is the assertion that the space-time evolution of the system looks essentially the same in all centre-of-mass-like frames, i.e. in all frames where the emergent excited nuclei are, shortly after collision , highly Lorentz contracted pancakes receding in opposite direction from the collision point at the speed of light.

The hydrodynamic equations also respect this symmetry. This leads to simple solutions of the hydrodynamic equations. In particular , for central collisions of large nuclei, the fluid

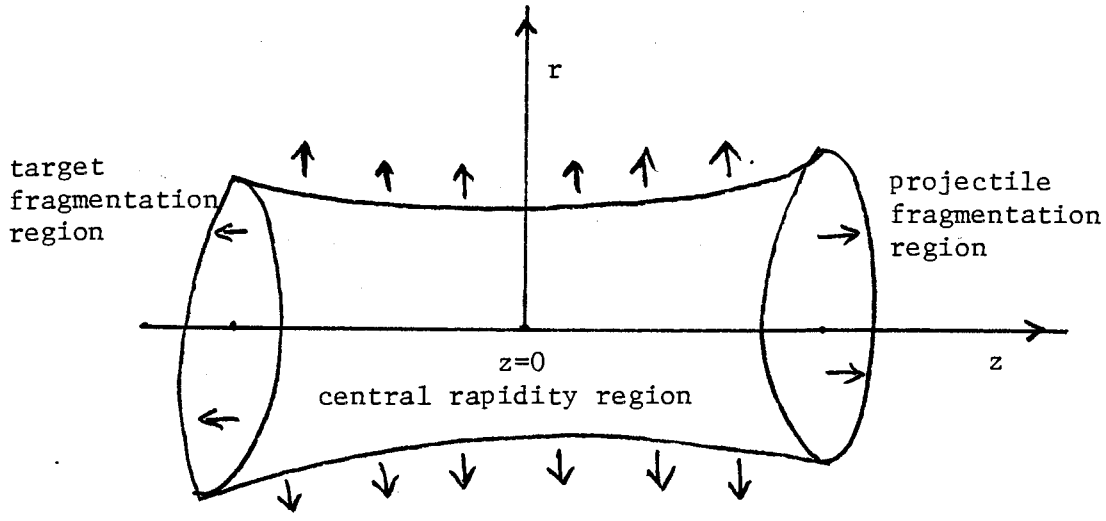

Fig. 2. Schematic view of a central collision of two highly Lorentz-contracted ultra-relativistic heavy ions in the c.m. frame, showing the target and projectile fragmentation regions, and the central rapidity regime.

expansion near the collision axis is longitudinal and homogeneous. The fluid midway between the receding pancakes remains at rest, while the fluid a longitudinal distance z from that midpoint moves with longitudinal velocity z/t , where t is the time elapsed since the pancake collided. This picture is modified at large transverse distances, comparable to the nuclear radii. At large transverse distances, the fluid will expand radially outward, cooling more rapidly than the fluid in the interior. One of the very important ingredients which goes into the space-time description of the plasma is the initial energy density ϵ_0.In first applications of hydrodynamics to hadronic collisions[15] it was assumed that in the centre of mass frame nuclear matter would be stopped, thus leading to gigantic energy densities. For a simple proton-proton collision with each proton having centre of mass energy, E , of 25GeV and taking into account the relativistic contraction in the longitudinal direction this leads to an energy density ϵ given by

$$\epsilon = 2E/[(4/3)\pi R_p^3 (m/E)] = 620 \text{GeV/fm}^3$$

for a proton radius of 0.8fm. The recent estimates[38,11] of about 2GeV/fm^3 differs from Landau's estimate because of the following two reasons:

(a) First of all it was realized[39] that nuclear matter has a minimum thickness. Taking a nucleus and boosting to an infinite momentum frame does not produce a nucleus with vanishing thickness. The nucleus even in an infinite momentum frame will

have finite thickness in the direction of motion and the thickness will be around 1fm. This can be understood in terms of the individual constituents of nucleons. In the infinite momentum frame a nucleon contains large amounts of wee partons, i.e. constituents with almost zero momentum.Therefore, this implies a limiting thickness for nucleons [39], which in turns implies a limiting thickness for a nucleus. This will modify Landau's original estimate drastically i.e.

$$\epsilon = 2E/[(4/3\pi)R_p^3] = 23\text{GeV/fm}^3$$

(b) The other factor which will reduce the initial energy density is the so called inside-outside cascade. As discussed before it will take a particle a proper time of τ_0 ,after the collision, before it will materialize. Therefore, slow moving particles will materialize before the fast moving particles because of the time dilation. It implies that it is possible for very fast moving particles to materialize outside the nucleus thereby limiting the number of collisions.

Bjorken's model takes into account both of the above mentioned effects. He estimated the initial energy density for a nucleus-nucleus collision by extrapolating the observed charged pion multiplicities in the central rapidity region in pp and $p\bar{p}$ collisions. For doing this, consider a thin slab of thickness 2d centered between the pancakes. Ignoring collisions between the produced hadrons, the energy contained within the thin slab is

$$E = A(dE/dy)\delta y = A(dE/dy)(1/2)2d/t \ .$$

Therefore, the energy density in the central region is

$$\epsilon \simeq A^{1/3}/[(1.2)^2\pi](dE/dy)(1/2t) = E/V,$$

where V is the volume. In the energy range $\simeq$ 30-270GeV per nucleon, the number of charged pions per unit of rapidity is $\simeq$ 2-3,[40] and one expects a total pion multiplicity density a factor 3/2 larger. The energy per unit of rapidity, assuming a final pion energy $\simeq$ 0.4GeV, is thus $dE/dy \simeq$ 1.2-1.8GeV.[41,42] Thus at the collision point one may estimate an energy density in the rest frame

$$\epsilon \simeq (0.3\text{-}0.4)\ A^{1/3}/t\ \text{GeV/fm}^3$$

For $t = \tau_0 \simeq$ 1fm/c, one gets

$$\epsilon_0 \simeq 2\text{GeV/fm}^3$$

If it is assumed that the matter at τ_0 consists of a gas of thermalized non-interacting quarks and gluons, then the temperature corresponding to the initial energy density of 2GeV/fm^3 is

$$T = (30/37\pi^2)^{1/4}\ (2\text{GeV/fm}^3)^{1/4} \simeq 200\text{MeV}.$$

The energy density and temperature in the central region estimated by using charged pion multiplicities is roughly of the same magnitude as obtained by using thermodynamics.

The criterion for the applicability of hydrodynamical laws is as follows: if the mean free path of particles is relatively short compared to the characteristic lengths of the system then one can apply the hydrodynamics. The mean free path of a particle is

$$\lambda = 1/(n_0\sigma)$$

where n is the density of excited quanta and σ is a mean scattering cross section in fm^2 . For cold nuclear matter n_0 = 0.15 nucleons/fm^3 and for a typical value of $\sigma = 4.0fm^2$, the mean free path is λ = 1.7fm. The increase in the energy density results in an increase of the total density of excited quanta which in turn implies a relatively short mean free path.

2.2.1 **HYDRODYNAMICAL LAWS:**

The laws of ideal relativistic fluid hydrodynamics are a direct consequence of conservation laws such as energy-momentum conservation, baryon number conservation etc. Most important of all is the law of energy-momentum conservation which is always true. In this respect the most important quantity is the energy-momentum tensor. The energy-momentum tensor can be defined by using the kinetic theory as [43,44]

$$T^{\mu\nu}(x) = \int p^{\mu}p^{\nu}f(x,p)d^3p/p_0 \ , \qquad (2.31)$$

where x is the position four vector, p is the momentum four vector, p_0 is the time component of the momentum four vector and f(x,p) is the one particle distribution function. The integral is taken over all the possible momentum states and the equilibrium form of one particle distribution function is

$$f(x,p) = 1/(\exp(E/T) \pm 1) \ . \qquad (2.32)$$

Using the most general homogeneous Lorentz transformation and assuming the isotropy of f(x,p) in p one gets

$$T^{\mu\nu}(x) = (\epsilon+P)u^{\mu}(x)u^{\nu}(x) - Pg^{\mu\nu} \ , \qquad (2.33)$$

where ϵ and P are the energy density and pressure respectively in the local rest frame. u^{μ} is the four velocity defined as

$$u^{\mu} = \gamma\ (1,\bar{v}) \qquad \gamma=(1-\bar{v}.\bar{v})^{-1/2}$$

The metric tensor $g^{\mu\nu}$(for cartesian coordinates) is defined as

$$g^{00}=-g^{11}=-g^{22}=-g^{33} = 1, \ g^{\mu\nu} = 0 \ \ \mu\neq\nu$$

The energy density ϵ and pressure P are defined as

$$\epsilon(\bar{x}) = \int \bar{E} f(\bar{x},\bar{p})d^3\bar{p} \ , \qquad (2.34)$$

$$P(\bar{x}) = \int \bar{p}^2/(3\bar{E})\ f(\bar{x},\bar{p})d^3\bar{p}\ , \qquad (2.35)$$

where all the barred quantities refer to the local rest frame. The energy-momentum tensor defined in eqn. (2.33) is a general tensor i.e. it is valid for any frame which is moving with a four velocity $u^\mu = \gamma(1,\bar{v})$ with respect to the lab frame. It consists of 16 components where T^{00} is the energy density and $T^{0i}(i=1,2,3)$ correspond to the flow of energy density and T^{ij} correspond to the momentum density. The rest of the components form a 3x3 stress or momentum flow tensor. $T^{\mu\nu}$ is symmetric tensor[44] i.e.

$$T^{i0} = T^{0i} \qquad T^{ij} = T^{ji}\ .$$

The symmetry of $T^{\mu\nu}$ is a consequence of the law of conservation of angular momentum. In the local rest frame where $u^\mu=(1,\bar{0})$. The energy-momentum tensor is a 4x4 diagonal matrix i.e.

$$\begin{bmatrix} \epsilon & 0 & 0 & 0 \\ 0 & P & 0 & 0 \\ 0 & 0 & P & 0 \\ 0 & 0 & 0 & P \end{bmatrix}$$

The energy-momentum tensor is isotropic in the local rest frame i.e. Pascal's law holds (what is equivalent to $\bar{T}^{11} = \bar{T}^{22} = \bar{T}^{33}$) . Beside all these properties, the energy-momentum tensor should

obey another condition i.e. the non-negativity of the trace

$$T^{\nu}_{\ \nu} \geq 0 \text{ or } T^{00}-T^{11}-T^{22}-T^{33} = \epsilon - 3P \geq 0 \ .$$

From eqn. (2.34) & (2.35) one gets

$$\begin{aligned} \epsilon - 3P &= \int [\bar{E} f(\bar{x},\bar{p}) - \bar{p}^2/\bar{E} \ . f(\bar{x},\bar{p})] d^3\bar{p} \\ &= m^2 \int f(\bar{x},\bar{p})/\bar{E} \ d^3\bar{p} \\ &= m^2/\langle \bar{E} \rangle , \end{aligned} \tag{2.36}$$

where m is the rest mass and brackets represent the statistical average. In the case of massless particles or for very large E, one gets from eqn. (2.36)

$$\epsilon - 3P = 0 \text{ or } P = 1/3 \ \epsilon \ , \tag{2.37}$$

which is the equation of state for an ultrarelativistic gas. This implies that defining the energy-momentum tensor uniquely is equivalent to defining an equation of state.

The hydrodynamical laws are essentially the same, when expressed mathematically, as the equation of continuity. In covariant formalism, for energy-momentum and baryon number conservation, it implies that the 4-divergence of $T^{\mu\nu}$ and J^{μ} should vanish i.e

$$\partial_{\mu} T^{\mu\nu} = 0 \qquad \mu, \nu = 0, 1, 2, 3 \tag{2.38}$$

$$\partial_{\mu} J^{\mu} = 0 \ , \tag{2.39}$$

where $J^{\mu} = \gamma(n, \bar{v}n)$ and n is the baryon number density in the local rest frame. In case of the central region, where the baryon number density is fairly small, one can drop eqn. (2.39). Therefore, here special emphasis is placed on eqn. (2.38) which is associated with the conservation of energy-momentum. The components of $T^{\mu\nu}$ are given explicitly in eqn.(2.33). If in addition to conservation of energy-momentum, one places the requirement that the expansion of the matter takes place slowly compared to natural collision times, that is slow enough that the expansion be reversible[38], then the entropy current is also conserved. This can be obtained directly from eqn. (2.38) by contracting with the four velocity u_{ν}

$$u_{\nu}\partial_{\mu}T^{\mu\nu} = 0$$

from eqn. (2.33)

$$u_{\nu}\partial_{\mu}\left[(\epsilon+P)u^{\mu}u^{\nu} - g^{\mu\nu}P\right] = 0 \ , \tag{2.40}$$

or, upon using the fact that u^{μ} is normalized to 1 one obtains

$$u^{\nu}\partial_{\nu}\epsilon + (\epsilon+P)\partial_{\nu}u^{\nu} = 0 \ . \tag{2.41}$$

Now by using the thermodynamic relations (2.12) and (2.14) in eqn. (2.41) one gets,

$$T\partial_{\nu}(u^{\nu}s) + \mu\partial_{\nu}(nu^{\nu}) = 0$$

one finds the strict conservation law

$$\partial_\nu(u^\nu s) = 0 \ , \qquad (2.42)$$

where s is the entropy density in the local rest frame. The entropy conservation in case of perfect fluids gives another reason, beside mathematical simplicity, for wishing to apply hydrodynamics only to perfect fluids. Entropy conservation relates particle multiplicities at early times to those at later times i.e.it allows us to reconstruct primeval distribution from those observed in the final state of collision. Another set of equations can be obtained by contracting eqn. (2.38) with the tensor $g^{\mu\nu}-u^\mu u^\nu$. This leads to

$$s[u^\nu\partial_\nu(u_\mu T)-\partial_\mu T]+ n[u^\nu\partial_\nu(u_\mu\mu)-\partial_\mu\mu] = 0 \ , \qquad (2.43)$$

2.2.2 ANALYTICAL SOLUTION OF HYDRODYNAMIC EQUATIONS:

The analytical solution of eqn. (2.38) can be obtained for some very simple cases. For Bjorken's type of picture of time evolution of the plasma, eqn. (2.38) can be solved analytically for one dimensional flow.[11] One can note the following important points associated to Bjorken's type of picture of time evolution of the plasma:

(1)It is applicable only to the central region where baryon number density is vanishingly small.

(2)It assumes the existence of a central plateau which implies that the initial conditions imposed on this region, after a

proper time $\simeq$ 1fm/c, are invariant with respect to Lorentz transformations.

(3)It assumes that the one dimensional flow should be a good approximation for times small compared to the radius of the nucleus:

$$t < 1.2A \simeq 7\text{fm/c for U.}$$

(4)It also assumes that the velocity in the longitudinal direction follows a simple scaling relationship i.e. $v = z/t$, where z is the distance measured from the point of collision in the longitudinal direction and t is the time elapsed after the collision.

The initial boundary conditions with the above assumptions for the longitudinal evolution of the quark-gluon plasma are,

$$\tau = \tau_0 = (t^2 - z^2) = \text{constant}$$

$$\epsilon = \epsilon_0 = \text{constant}$$

Therefore, in this case hydrodynamic eqn. (2.40) simplifies to

$$d\epsilon/d\tau = -(\epsilon+P)/\tau \ . \qquad (2.44)$$

Also eqn. (2.42) for entropy conservation reduces to

$$ds/d\tau = -s/\tau,$$

$$s(\tau) = s_0 \, (\tau_0/\tau) \, ,$$

where s_0 is the entropy density at proper time τ_0 . For an ideal relativistic fluid type of equation of state, one gets from eqn. (2.44)

$$d\epsilon/d\tau = -(4/3)(\epsilon/\tau)$$

where p is replaced by $(1/3)\epsilon$. Finally integrating the above equation gives

$$\epsilon(\tau) = \epsilon_0(\tau_0/\tau)^{4/3} \, . \qquad (2.45)$$

In this case $\epsilon \, \alpha \, T^4$ and hence the temperature drops slowly, as $\tau^{-1/3}$. One can also determine the differential equation for the time dependence of temperature of the fluid. From eqn. (2.44), with $\epsilon = \epsilon(P)$ and $P = P(T)$, one gets

$$d\epsilon/d\tau = (d\epsilon/dP)(dP/dT)(dT/d\tau) = -(\epsilon+P)/\tau$$

Also

$$\epsilon+P=Ts, \; dP/dT=s, \; d\epsilon/dP = 1/v_s^{\,2}$$

where v_s is the velocity of sound. Finally one gets

$$dT/d\tau = -v_s^{\,2}/\tau \, . \qquad (2.46)$$

One can now exploit the special form of the scaling solution to discuss also the behaviour in the transverse direction.[38] Since the scaling solution is invariant under Lorentz boosts along the longitudinal direction it is sufficient to go to one point where the equations are simple, z=0, and construct the solution in transverse direction. In the cylinderical coordinates with the beam direction as the z-axis the four velocity is given by

$$u_\mu = \gamma(1, v_r, v_z, 0) \qquad \gamma=(1-v_r^2-v_z^2)^{-1/2}$$

if there is azimuthal symmetry. At z=0 this reduces to $u_\mu=\gamma(1,0,v_r,0)$ just as in the case of the longitudinal motion. In case of zero chemical potential and at z = 0, the entropy eqn. (2.42) and eqn. (2.43) reduces to

$$(1/v_s)\partial \ln T/\partial t + v_r v_s \partial\gamma/\partial t + (v_r/v_s)\partial T/\partial r + v_s \partial\gamma/\partial r + v_r v_s/r + v_s/t = 0, \qquad (2.47)$$

$$v_r \partial \ln T/\partial t + \partial\gamma/\partial t + \partial \ln T/\partial r + v_r \partial\gamma/\partial r = 0. \qquad (2.48)$$

Addition and substraction of these two equations leads to the hydrodynamic equations of motion in the radial direction

$$\partial/\partial t(1/v_s \ln T \pm \gamma) + [(v_r \pm v_s)/(1 \pm v_r v_s)]\, \partial/\partial r(1/v_s \ln T \pm \gamma) + (v_r v_s/r)(1 \pm v_r v_r) + (v_s/t)(1 \pm v_r v_s) = 0 . \qquad (2.49)$$

The important velocity in eqn. (2.49) is the velocity relative

to the speed of sound. The first two terms in this equation correspond to a simple wave equation and last two terms in eqn. (2.49) are the deriving terms. A class of solutions of eqn. (2.49) also corresponds to simple rarefaction waves propagating into the fluid. Rarefaction waves are obtained by looking for the solutions independent of the proper time τ. The following approximate rarefaction wave solution for eqn. (2.49) was obtained by Baym[38]

$$y \simeq y_{rad} \pm y_s$$

where

$$y_{rad}=1/2\ln[(t+r)/(t-r)]$$

CHAPTER 3

NUMERICAL SOLUTION OF HYDRODYNAMIC EQUATIONS

This chapter includes a detailed discussion of the model used for initialisation of the quark-gluon plasma and details of the numerical method used here to study the time evolution of the hydrodynamically expanding plasma. The kind of initialisation used here is formulated by using a parton cascade model[45] based on perturbative QCD. Such a formulation will have obvious limitations in its applicability to such non-perturbative problems as pion multiplicities and entropy production in the hadronization region. Nevertheless, it involves more physics than the models being used by other authors[46-48] for generating the initial conditions for the plasma. Once the initial conditions are generated for the plasma, the hydrodynamic equations can be solved numerically by using an appropriate finite difference scheme. There are number of methods available for solving such equations numerically[48-50]. The method used here is the two-step Lax-Wendroff method[51,52] and it is chosen because of the following two reasons:

(a) it centres the integration in the time and space variables properly;

(b) it is simple and requires less storage and computer time than other available methods.

3.1 INITIALISATION:

The model used here consists of independent parton-parton scattering based on lowest order of QCD. The parton trajectories in coordinate space are classical. The collisions involved here are central and viewed in the centre-of-mass frame with equal target and projectile mass (A = 50 + A = 50). The centre-of-mass energy is $\sqrt{s}$ = 20GeV/A and all the results obtained here are for zero impact parameter. Each nucleon is represented by quarks and gluons, each carrying a fraction x of the nucleon's centre of mass momentum. The fractional momentum is distributed according to [53]

$$xq(x) = 1.10(1+3.7x)(1-x)^{3.19}, \tag{3.1}$$

$$xg(x) = 2.62(1+3.5x)(1-x)^{5.9}, \tag{3.2}$$

where q(x)dx and g(x)dx are the number of quarks or gluons in an x interval dx. The integration of the above equation over the whole x range will clearly be an infinite number of partons. Equation (3.1) and (3.2) has a singularity at x=0, to avoid the singularity as x→0, a cutoff is put in around $x_0 \simeq 0.02$. The cutoff is determined by demanding

$$\int_{x_0}^{1} q(x)dx = 3, \tag{3.3}$$

$$\int_{x_0}^{1} g(x)dx = 5, \tag{3.4}$$

and is slightly different for quarks and gluons. One could choose a value of x_0 closer to zero and follows the trajectories of even more partons. The advantage of this is better statistics but, this would slow the code down considerably and not necessarily provide that much improvement in accuracy for calculating processes involving hard partons. The antiquarks are omitted from the initialisation because for $x_0 \simeq 0.2$, the corresponding integral over the antiquark distribution gives a value much less than 1. The fractional momenta to be used in the initialisation were stored in a lookup table with 200 entries. The entries x_i are determined by calculating the first 200 values of from which

$$200 \int_1^{x_i} q(x)dx \ , \tag{3.5}$$

gives an integral value. The code could then choose randomly from among these values during the initialisation. The partons were also assigned a momentum in the tranverse direction. This is being done by using a normal distribution with variance of $180 \mathrm{MeV}/c^{54}$.

The coordinate space distribution was handled as follows: first the nucleon positions were assigned randomly within the spherical nucleus, and then the parton positions assigned randomly within a sphere of radius 1fm about the nucleon position. All of these coordinates were then Lorentz contracted as viewed from the centre-of-mass frame. The parton coordinates

were shifted around their assigned positions according to a normal distribution of variance equal to the reduced de Broglie wavelength squared. Thus, the density of soft partons is lower than that of hard partons.

The partons follow classical straightline trajectories until they undergo a collision. The method used here to determine that a particular pair of partons undergoes a collision or not is simple: the three dimensional dot product of the relative position and momentum of each parton pair was evaluated at the beginning and end of each time step (assuming no collision). If the product changed sign in the step, a collision potentially had occured. If $\sqrt{s}$ (where s,t,u are the usual Mandelstam variables) involved in the collision were less than 2GeV, the collision was discarded. A check was made to see if the distance of closest approach was within $\sqrt{\sigma/n}$, the cross section σ being defined by

$$\int_0^\infty [d\sigma/dt]dt$$

with $d\sigma/dt$ defined below.

The cross sections were taken from lowest order of QCD results for 2→2 scattering[55]. For simplifying the algorithm the most singular part in t of the differential cross section is taken i.e.

$$d\sigma/dt \quad \alpha \quad t^{-2}$$

One can find a value for t such that for a random number χ between 0 and 1, the following expression could be inverted analytically:

$$\chi=\bar{\int}_t^\infty [d\sigma/dt]dt/\bar{\int}_0^\infty [d\sigma/dt]dt \ . \qquad (3.6)$$

The cutoff in t was determined by putting a cutoff of 1/2 GeV/c in transverse momentum.

The code also takes into account the scattering of off shell partons (i.e.inelastic collisions). Such off shell scatterings can not be omitted beacuse then the calculations would be unrealistic, the nuclei would be much too transparent to each other. In this code once a parton has been scattered off shell, it decays to two collinear zero mass partons with life time equal to $\bar{h}/\alpha_s m$, where α_s is the strong coupling constant. The energy of parent parton is divided into fractions z and 1-z which is carried by daughters at the time step when it decays. The fractions are distributed according to the Altarelli-Parisi splitting functions[56]

$$P_{q/q} = 4/3(1+z^2)/(1-z), \qquad (3.6)$$

$$P_{G/G} = 6(1-z+z^2)/[z(1-z)], \qquad (3.7)$$

$$P_{G/q} = N_f/2[z^2+(1-z)^2], \qquad (3.8)$$

where $P_{i/j}$ is the distribution of partons of type j, produced in the decay of parton of type i, carrying off an energy fraction

z. Lastly, the QCD constant α_s was set equal to 1/2 throughout.

Once the events have been generated by the simulation, the next step is to bin the particles properly. To do this a computer code has been written which generates a space mesh of size 16x16x16, which is equivalent to 4096 fluid cells. The cell width in the longitudinal direction is of the size 0.5fm whereas in transverse directions it is 1fm, giving a volume of each cell of $0.5fm^3$. The reason for a smaller width size in the longitudinal direction than in the transverse directions is because the cells are highly Lorentz contracted in this direction. For determining the motion of fluid cells, the procedure used here is to contruct a energy-momentum tensor for the N particles in each cell via [43]

$$T^{\mu\nu} = (1/V)\sum_{n=1}^{N} P_n^{\mu} P_n^{\nu}/E_n, \qquad (3.9)$$

where V is the volume of the fluid cell. The velocity components of each cell are determined by using the fact that momentum densities should vanish, $\tilde{T}^{0i} = 0$, in the local rest frame of the cell. The transformed tensor is defined by

$$\tilde{T}^{0i} = \Lambda^0_{\mu}\Lambda^i_{\nu}T^{\mu\nu} \qquad i=1,2,3 \qquad (3.10)$$

where Λ^{μ}_{ν} is the pure Lorentz boost defined as

$$\Lambda^0_0 = \gamma \qquad \Lambda^i_0 = \Lambda^0_j = \gamma v_i$$

$$\Lambda^i_j = \delta_{ij} + v_i v_j(\gamma-1)/\ \mathbf{v}^2$$

By substituting the above equations in equation (3.10) one gets the following expressions for three velocity components:

$$v_1=-(T^{10}+v_2T^{12}+v_3T^{13})/\ (DENO+T^{11})\ , \tag{3.11}$$

$$v_2=-(T^{20}+v_1T^{12}+v_3T^{23})/\ (DENO+T^{22})\ , \tag{3.12}$$

$$v_3=-(T^{30}+v_1T^{13}+v_2T^{23})/\ (DENO+T^{33})\ , \tag{3.13}$$

where

$$\begin{aligned} DENO\ =&\gamma T^{00}+(\gamma+(\gamma-1)/v^2)\ (v_1T^{10}+v_2T^{20}+v_3T^{30})+\\ &(\gamma-1)/v^2[v_1^2T^{11}+v_2^2T^{22}+v_3^2T^{33}+\\ &2(v_1v_2T^{12}+v_1v_3T^{13}+\ v_2v_3T^{23})] \end{aligned} \tag{3.14}$$

The above equations can be solved for different components of velocity by using a simple one-point iteration procedure. This binning code calculates the initial energy density ϵ in the local rest frame of the cell by using the equation (3.10). The pressure P of a cell is determined by using an equation of state for an ideal relativistic fluid i.e $P=(1/3)\epsilon$. The energy density ϵ, pressure P and the hydrodynamic velocity $\bar{v}$ of each cell is stored in a file, which is then used as the initial conditions for the numerical solution of hydrodynamic equations.

3.2 THE TWO-STEP LAX-WENDROFF SCHEME:

In this section a numerical method of solving the hydrodynamical equations is presented. The hydrodynamical equations for the time evolution of the quark-gluon plasma are given by using the equation (2.54),

$$\partial T^{00}/\partial t + \partial T^{10}/\partial x + \partial T^{20}/\partial y + \partial T^{30}/\partial z = 0, \qquad (3.15)$$

$$\partial T^{01}/\partial t + \partial T^{11}/\partial x + \partial T^{21}/\partial y + \partial T^{31}/\partial z = 0, \qquad (3.16)$$

$$\partial T^{02}/\partial t + \partial T^{12}/\partial x + \partial T^{22}/\partial y + \partial T^{32}/\partial z = 0, \qquad (3.17)$$

$$\partial T^{03}/\partial t + \partial T^{13}/\partial x + \partial T^{23}/\partial y + \partial T^{33}/\partial z = 0, \qquad (3.18)$$

where first of these equations is associated with the law of conservation of energy and the last three equations are associated with the law of conservation of momentum. The above equations consist of first order hyperbolic partial differential equations and they are non-linear. The problem posed by the numerical solution of such equations is classified in a broad class of problem i.e. the initial-value problem. An initial-value problem is the one where the state of system is completly specified at some initial time with the help of certain variables associated with it. Then, with the help of a differential equation or a set of differential equations these variables evolve in time. In the case of the hydrodynamical expansion of the quark-gluon plasma, variables of interest are the energy density ϵ, pressure P and the hydrodynamic velocity $\bar{v}$.

In the code described here, these equations are solved at each point of a cubical mesh, where each point on the mesh is a representaive of some fluid cell. The mesh points or fluid cells at the boundaries are treated differently than the interior mesh points. [1] Cartesian coordinates are being used, because these coordinates are the most appropriate for impact parameter averaging problems. For problems with non-zero impact parameter, the more appropriate coordinates for heavy ion collisions is either cylinderical or spherical.[44] But the use of spherical or cylinderical coordinates give rise to another problem i.e. the hydrodymaical equations can no longer be written in a conservative form(i.e. a form similar to the equation of continuity).[50] Another problem, which arises due to the use of spherical or cylinderical coordinates is the appearance of the additional term, $r\partial P/\partial r$. When such a term is approximated on a computer generated mesh, the result is an unstable scheme at the axis r=0.[57]

The time evolution of the variables ϵ, P, $\bar{v}$ associated with a particular fluid cell is dependent upon the variables associated with the neighboring cells. This fact is taken into account by using the central difference scheme. It means the derivative at a mesh point i is calculated by using the values of the variable at mesh points i+1 and i-1. This procedure is used for all the interior mesh points. The mesh points at the boundaries, for which $i=i_{max}$, a backward difference scheme is

---

[1] In here the term mesh point or a fluid cell will be used interchangably.

used i.e. the derivaties at i are evaluated by using the values of the variables at mesh points i and i-1. The mesh points for which $i=i_{min}$, a forward difference scheme is being used i.e. the derivatives at i are being evaluated by using the values of the variables at mesh points i and i+1.

$T^{\mu\nu}$ used in the above equations is defined according to the equation (2.49) as,

$$T^{\mu\nu} = (\epsilon+P)u^{\mu}u^{\nu} - g^{\mu\nu}P \ .$$

Before discussing the numerical solution of the above equations we will write down these equations in a manner which is similar to the equation of continuity i.e.

$$\partial\rho/\partial t + \nabla.\rho\bar{v} = 0$$

where ρ is the space density of some quantity and $\rho\bar{v}$ is the flux of this quantity. For doing that one can define the following variables,

$$E = \gamma^2(\epsilon+P) - P \ , \qquad (3.19)$$

$$P_x = \gamma^2(\epsilon+P)v_x, \qquad (3.20)$$

$$P_y = \gamma^2(\epsilon+P)v_y \ , \qquad (3.21)$$

$$P_z = \gamma^2(\epsilon+P)v_z \ , \qquad (3.22)$$

the variables E, P_x, P_y and P_z represent the energy density and

the momentum density of a fluid cell in a frame with respect to which it is moving with a velocity $\bar{v}$. ϵ and P are the energy density and the pressure in the local rest frame of the fluid cell. Now all the components of tensor $T^{\mu\nu}$ can be expressed in terms of E, P_x, P_y and P_z with the help of equations (2.49) and (3.19-3.22) as follows:

$$T^{00} = E,\ T^{10} = (E+P)v_x,\ T^{20} = (E+P)v_y$$

$$T^{30} = (E+P)v_z,\ T^{01} = P_x,\ T^{11} = v_xP_x+P$$

$$T^{21} = v_yP_x,\ T^{31} = v_zP_x,\ T^{02} = P_y$$

$$T^{12} = v_xP_y,\ T^{22} = v_yP_y+P,\ T^{32} = v_zP_y,\ T^{03} = P_z$$

$$T^{13} = v_xP_z,\ T^{23} = v_yP_z,\ T^{33} = v_zP_z+P\ . \qquad (3.23)$$

Using equation (3.23) one can write equations (3.15-3.18) as follows:

$$\partial E/\partial t+\partial[v_x(E+P)]/\partial x+\partial[v_y(E+P)]/\partial y+\partial[v_z(E+P)]/\partial z=0 \qquad (3.24)$$

$$\partial P_x/\partial t+\partial[v_xP_x+P]/\partial x+\partial[v_yP_x]/\partial y+\partial[v_zP_x]/\partial z=0 \qquad (3.25)$$

$$\partial P_y/\partial t+\partial[v_xP_y]/\partial x+\partial[v_yP_y+P]/\partial y+\partial[v_zP_y]/\partial z=0 \qquad (3.26)$$

$$\partial P_z/\partial t+\partial[v_xP_z]/\partial x+\partial[v_yP_z]/\partial y+\partial[v_zP_z+P]/\partial z=0. \qquad (3.27)$$

The method used here for solving the above set of equations is the two-step Lax-Wendroff method.[52] This method has second order accuracy in time and space variables. Before discussing the above numerical method, a few words will be said about the general formulation of the initial-value problem. To do this a

simple differential equation in one dimension is considered. Most of the ideas applicable to a one-dimensional problem, can easily be generalized to a multi-dimensional problem.

Consider a simple differential equation

$$dx/dt = Ix$$

where I is a non-linear integral operator. $x(r,t)$ is a state vector of the system which defines the system over a space domain $R=R(r)$ and for all time. If $x=x^0$ is defined at time $t=0$ then the above differential equation determines $x(r,t)$ for all time, provided the form of I is known. For solving such a differential equation on the computer, one needs to define a discrete space-time mesh. Once this has been done, the time integration of the above equation relates the state vectors x^{n+1} and x^n of the system at adjacent time points t^{n+1} and t^n: [2]

$$x^{n+1} = x^n + \int_{t^n}^{t^{n+1}} Ixdt' \quad . \tag{3.28}$$

The integral on the right-hand side of equation (3.28) cannot be evaluated exactly, since the vector $x(t')$ is not known for all time t' in the interval, $t^n \leq t' \leq t^{n+1}$. Hence the essential finite difference approximation is introduced by assuming that for small time steps, $\Delta t = t^{n+1}-t^n$, the integrand in equation (3.28) may be approximated by a finite Taylor series expansion,

---

[2] In here a particular time point is written as a superscript to the variable and a particular space point as a subscript to the variable.

$$x^{n+1}=x^n+\int_{t^n}^{t^{n+1}} \{\Sigma[d^r(Ix)/dt^r]\ t'^r/r!\ +O(t^p\}dt'$$

and after integrating the right-hand side:

$$x^{n+1} = x^n +\Sigma[d^{r-1}Ix/dt^{r-1}](\Delta t)^r/r!\ +O(\Delta t^{p+1}) \ , \quad (3.29)$$

where p is the order of accuracy in the time step Δt to which the integration scheme is carried out. Usually in a finite difference scheme higher order terms than the second are not included. In practice second-order accuracy can be achieved by using the variables at previous time levels, or by defining the intermediate time, or by using the unknown variable at the time step ahead. The above integration scheme, with second-order accuracy and by using the variables at the time step ahead, takes the following form:

$$x^{n+1} = x^n +Ix^n(1-\delta)\Delta t + Ix^{n+1}\delta\Delta t$$

where δ is the interpolation parameter and second-order accuracy is only maintained when δ =1/2. In the special case when δ =0, the new state u^{n+1} is defined explicitly by the known state x^n at the previous time step. In this event method is said to be explicit, while on the other hand if $\delta \neq 0$ the method is said to be implicit.

The method used in this code is an explicit method and second-order accuracy in time is achieved by defining the intermediate time. Equations (3.24-3.27) have a general form of sort,

$$\partial u/\partial t + \partial F_x/\partial x + \partial F_y/\partial y + \partial F_z/\partial z = 0 \ , \qquad (3.30)$$

where u is the quantity of interest, F_x, F_y and F_z are the fluxes of u in x, y and z-directions respectively. First an intermediate or half time step is defined at which the values of all dependent variables [3] are calculated. This is being done as follows: [52]

$$u^{n+1/2}_{i,j,k} = 1/6[u^n_{i+1,j,k}+u^n_{i-1,j,k}+u^n_{i,j+1,k}+u^n_{i,j-1,k}$$

$$+u^n_{i,j,k+1}+u^n_{i,j,k-1}] -\Delta t/(4\Delta x)[F^n_{x,i+1,j,k} -F^n_{x,i-1,j,k}$$

$$+F^n_{y,i,j+1,k} -F^n_{y,i,j-1,k} +F^n_{z,i,j,k+1} -F^n_{y,i,j,k-1}]$$

. $\qquad (3.31)$

Obviously equation (3.31) is valid only for the interior mesh points. For a mesh point at the boundaries i+1, j+1, and k+1 may correspond to points which are outside the space mesh defined for the problem. In such a case, code bypasses equation (3.31) and uses the following equation:

$$u^{n+1/2}_{N,j,k}=1/6[u^n_{N,j,k}+u^n_{N-1,j,k}+u^n_{N,j+1,k}+u^n_{N,j-1,k} +$$

$$u^n_{N,j,k+1}+u^n_{N,j,k-1}]-\Delta t/(2\Delta x)[F^n_{x,N,j,k} -F^n_{x,N-1,j,k}]-$$

$$\Delta t/(4\Delta x)[F^n_{y,N,j+1,k} -F^n_{y,N,j-1,k} +$$

$$F^n_{z,N,j,k+1} -F^n_{z,N,j,k+1}] \ , \qquad (3.32)$$

---

[3] In here u, F_x, F_y and F_z are referred as dependent variables whereas x, y, z and t are taken as independent variables.

at a boundary surface. The subscript N appearing in the above equation correspond to the boundary. It can take only two possible values i.e i_{max} or i_{min} when considered for the boundary in x-direction.[4] For a cubical mesh there are number of different boundary conditions such as boundary surfaces, boundary lines and boundary points. Equation (3.32) corresponds to a boundary surface and in the code we have six such equations corresponding to six surfaces of the cubical mesh. Similarly, there are 12 boundary lines which correspond to the subscripts of the form (N,N,k) and there are eight boundary points (N,N,N). For all these boundaries, equations similar to the equation (3.32) are being used with little changes. All of them are not written here explicitly because it is too cumbersome to write them down.

Next, from equations (3.24-3.27) and (3.31-3.32) one gets the values of E, P_x, P_y and P_z at the intermediate time step and then these values are used to define the fluxes at the intermediate time. But, here all fluxes are defined in terms of E, P_x, P_y, P_z, v_x, v_y, v_z and P, and yet we do not know the values of v_x, v_y, v_z and P at the intermediate time. This can be accomplished with the help of equations (3.19-3.22) and the equation of state. Equations (3.19-3.22) reduce to

$$E = (4/3)\gamma^2\epsilon - (1/3)\epsilon \ , \tag{3.33}$$

$$P_x = (4/3)\gamma^2\epsilon v_x \ , \tag{3.34}$$

---

[4]The subscripts i, j, and k will refer to x, y, and z-directions respectively.

$$P_y = (4/3)\gamma^2 \epsilon v_y \ , \tag{3.35}$$

$$P_z = (4/3)\gamma^2 \epsilon v_z \ . \tag{3.36}$$

The above set of equations can be solved simultaneously for the unknowns ϵ, v_x, v_y, and v_z by using the known variables E, P_x, P_y, and P_z at the intermediate time step. This is being done by solving the following equation, which is obtained from equations (3.33-3.36),

$$z = (3+z)^2 \bar{P}.\bar{P}/(16E^2) \ , \tag{3.37}$$

where $z=\bar{v}.\bar{v}$ and $\bar{P}.\bar{P}$ are the squares of the magnitude of velocity and momentum vectors respectively. Equation (3.37) can be solved for z by iteration and the iteration procedure will be stable if dG(z)/dz is less than 1, where G(z) is equal to the right-hand side of equation (3.37). The condition that $dG(z)/dz < 1$ is satisfied, if $z < 1$ and $\bar{P}.\bar{P} < E^2$. For hydrodynamical equations both conditions are satisfied because $\bar{v}$, the hydrodynamical velocity of a fluid cell, can never exceed the velocity of light($c = 1$). $\bar{P}$ which is the total momentum density of the fluid cell is always less than or equal to E. In the code, however, some difficulties occur for the fluid cells at the edges where $z > 1$. Such a circumstance is physically impossible, corresponding to speeds exceeding that of light. This situation can be anticipated whenever $\bar{P}.\bar{P} > E^2$. A situation like this is always associated with stagnation of the fluid relative to the computational mesh, in which case the energy flux vanishes but

the momentum flux remains appreciable. To avoid this difficulty, the code bypasses the iteration procedure and lets the cell move with the same speed as the neighbouring cells.

Once the value of z is known at the intermediate time step, one can calculate $\gamma = 1/(1-z)^{1/2}$ and then ϵ, v_x, v_y and v_z can be obtained for the time $t^{n+1/2}$, by using equations (3.33-3.36) respectively. Using the new values of these variables, all the fluxes are updated for the time $t^{n+1/2}$. Finally, the value of variable u is calculated for the time step t^{n+1}, by using the following equation:

$$u^{n+1}_{i,j,k} = u^{n}_{i,j,k} - \Delta/(2\Delta x)[F^{n+1/2}_{x,i+1,j,k} - F^{n+1/2}_{x,i-1,j,k} + F^{n+1/2}_{y,i,j+1,k} - F^{n+1/2}_{y,i,j-1,k} + F^{n+1/2}_{z,i,j,k+1} - F^{n+1/2}_{z,i,j,k-1}] \quad . \tag{3.38}$$

The above equation is only valid for the interior mesh points, therefore, again for the mesh points at the boundaries equations similiar to the equation (3.32) are being used. Finally, using equations (3.33-3.37) the values of ϵ, v_x, v_y and v_z are calculated for the time step t^{n+1}. Then the same procedure is being used for all subsequent time steps.

One of the most important requirements for the numerical method is stability i.e. the solution obtained should be bounded. For a multi-dimensional two-step Lax-Wendroff method the stability condition is[51]

$$\Delta t \leq \Delta/(\sqrt{3}|\bar{v}|) \ , \qquad (3.39)$$

where $\bar{v}$ is the fastest propagation velocity anywhere on the space mesh. This condition is not surprising because one is required to choose a time step smaller than the smallest characteristic physical time in the problem. In this code, the size of time step is taken to be 0.1fm and the size of space step in x and y-directions is 1.0fm, whereas in the z-direction it is 0.5fm. These numbers obviously satisfy the equation (3.39) and ensures the stability of the numerical method used here.

3.3 **RESULTS:**

Before discussing our results, we say a few words about the computer generated initial conditions. As mentioned earlier, the hydrodynamical description is valid only if the system is in local thermal equilibrium. Because of the limited number of particles in each fluid cell we can not check the momentum spectra of the particles in each direction to determine how close to thermal equilibrium the distribution is. However, a quick check of the computer generated initial distribution is to calculate the ratio of the spatial-diagonal components of the energy-momentum tensor in the local rest frame of the system. Obviously, this ratio should be unity if the momentum distribution is istropic. In our code, the components T^{11}, T^{22} and T^{33} of the energy-momentum tensor are first transformed to the local rest frame of a fluid cell and then the ratio of

$\tilde{T}^{33}/\tilde{T}^{11}$ is calculated. A plot of this ratio versus the radius vector is shown in Fig. (3)(the radius vector of a fluid cell is defined as the distance from the origin of the space mesh). For most of the fluid cells, this ratio is between 0.5 and 1.75. The average ratio for the initial distribution is 1.57 where the average is taken over all fluid cells.

In Fig. (4) the behaviour of energy density with respect to time is shown. It is a log log plot and a regression line is fit to the data. The slope of this line is -5/3 i.e. ϵ is proportional to $t^{-5/3}$. In case of simple longitudinal expansion[11] the energy density is proportional to $t^{-4/3}$. The reason why we get a larger value for the time exponent is as follows: our model includes both the longitudinal and the transverse expansion of the quark- gluon plasma as compared to the model used in reference 11 where only the longitudinal expansion is taken into account. At this point we would like to mention that earlier it was calculated by Bjorken[11] that after t $\simeq$ 3-4fm/c, for U-U collisions, no more than 50% of the fluid moves one dimensionally. In our case the motion of the fluid is not one dimensional since the beginning. It can be seen in Fig. (4) where the energy density falls off with time as $t^{-5/3}$ from the beginning. This is possibly a result of the intermediate mass number of nuclei we are looking at.

In Fig. (5), (6), (7) and (8) we have plotted the longitudinal distributions of the energy density, temperature, longitudinal velocity and the transverse velocity. In all these

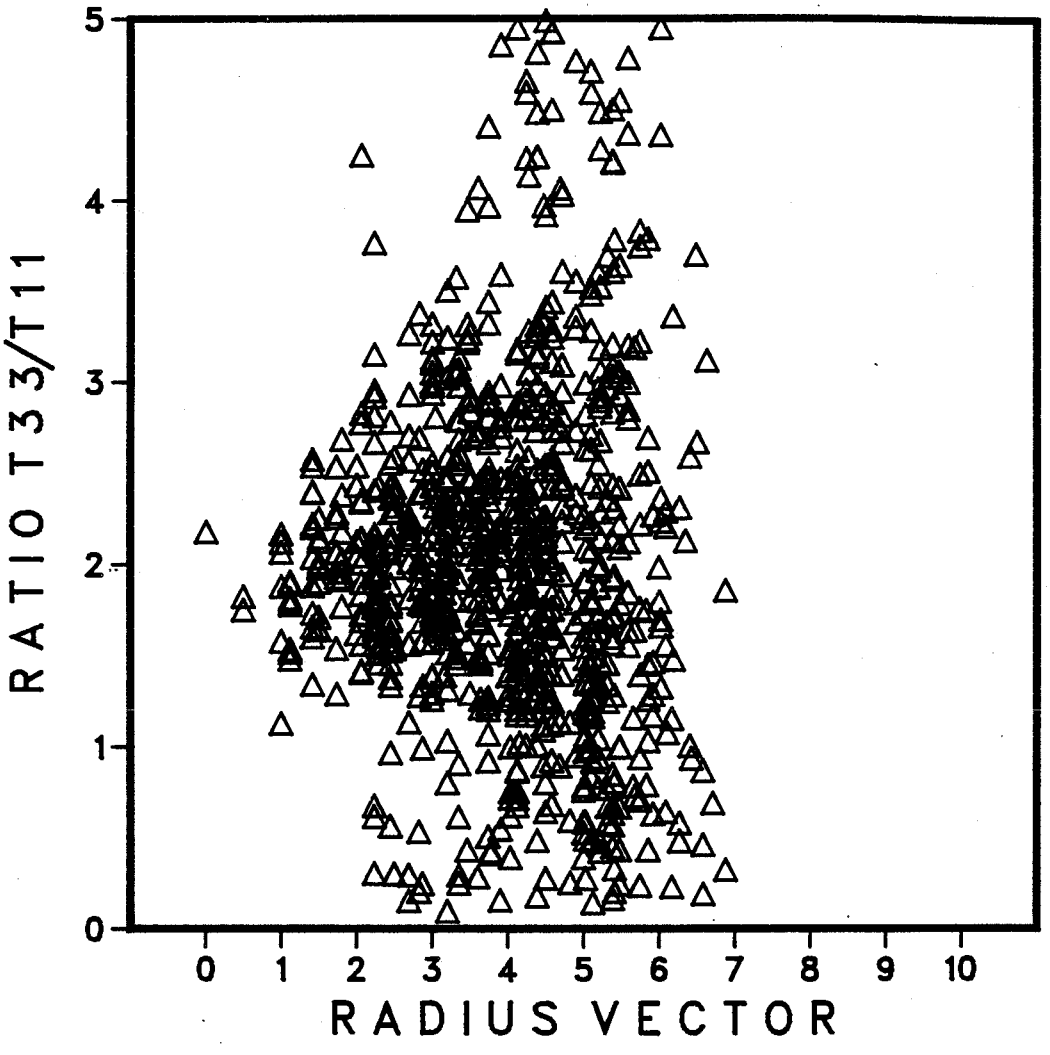

FIG.3. The ratio of T33 to T11 is plotted versus the radius vector. The radius vector for a fluid cell is defined as the distance from the origin of space mesh.

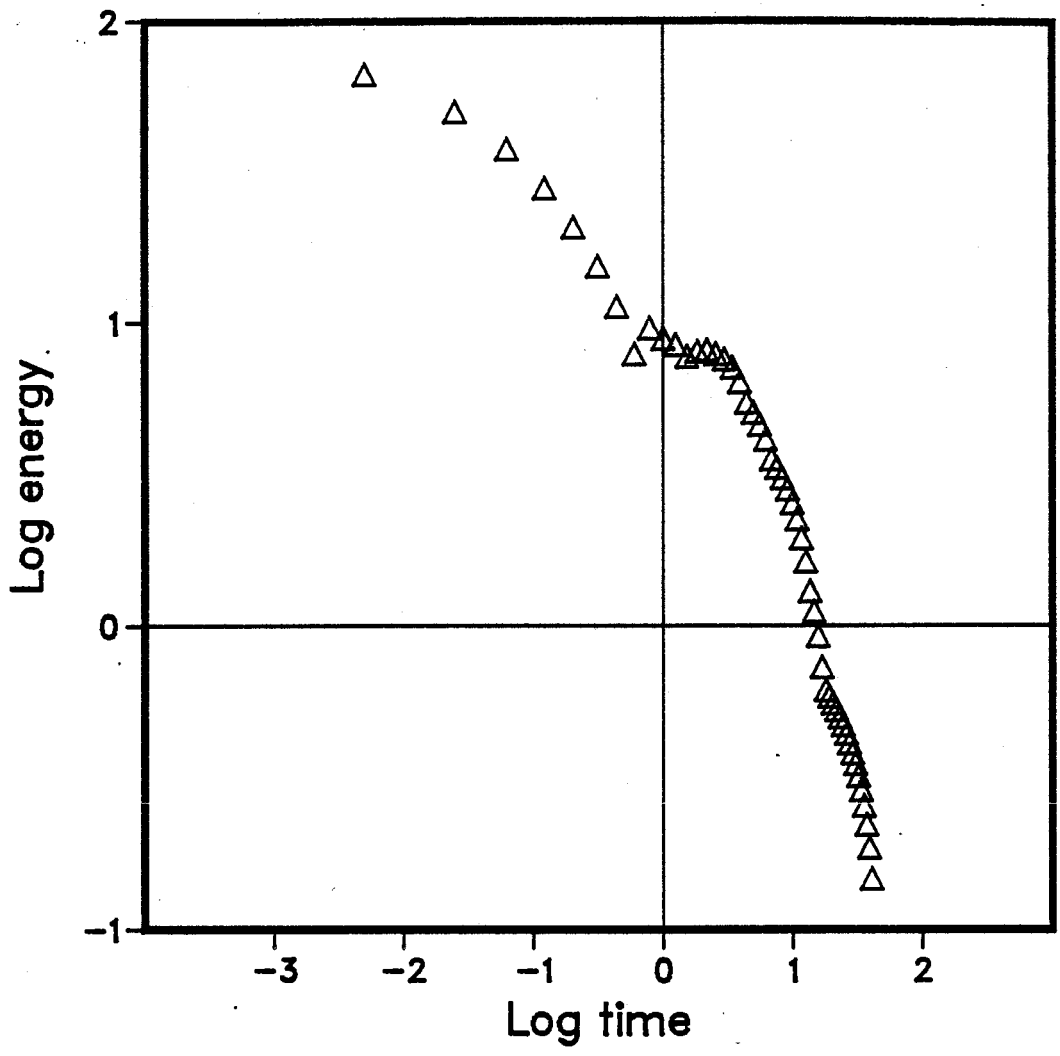

Fig. 4. The log of energy density plotted versus the log of time for the fluid cells at the center of the computer generated mesh.

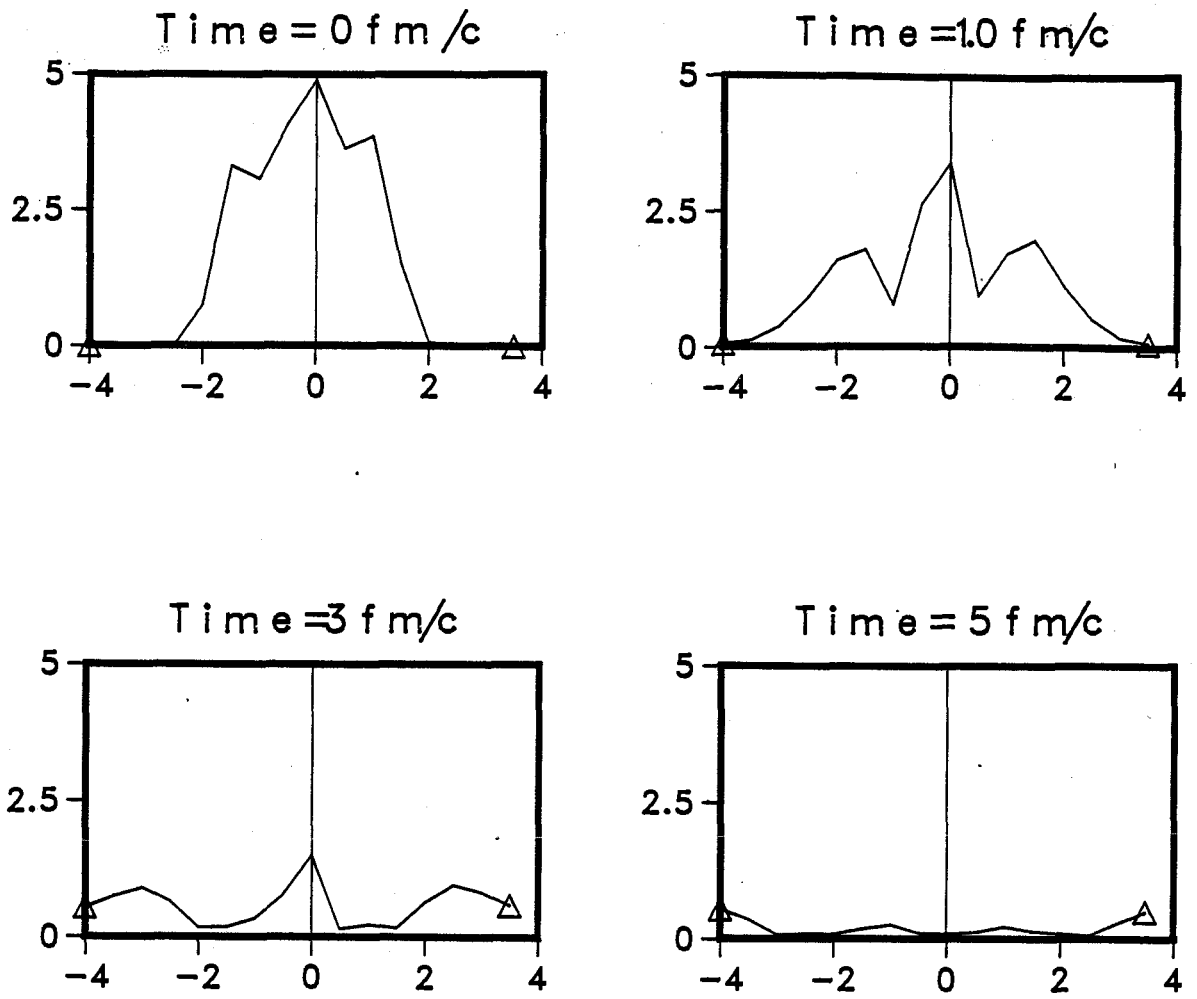

Fig. 5. The longitudinal distribution of the energy density at times 0, 1, 3 and 5fm/c. The units of vertical axis is GeV per cubic fm and the units of horizontal axis is fermi.

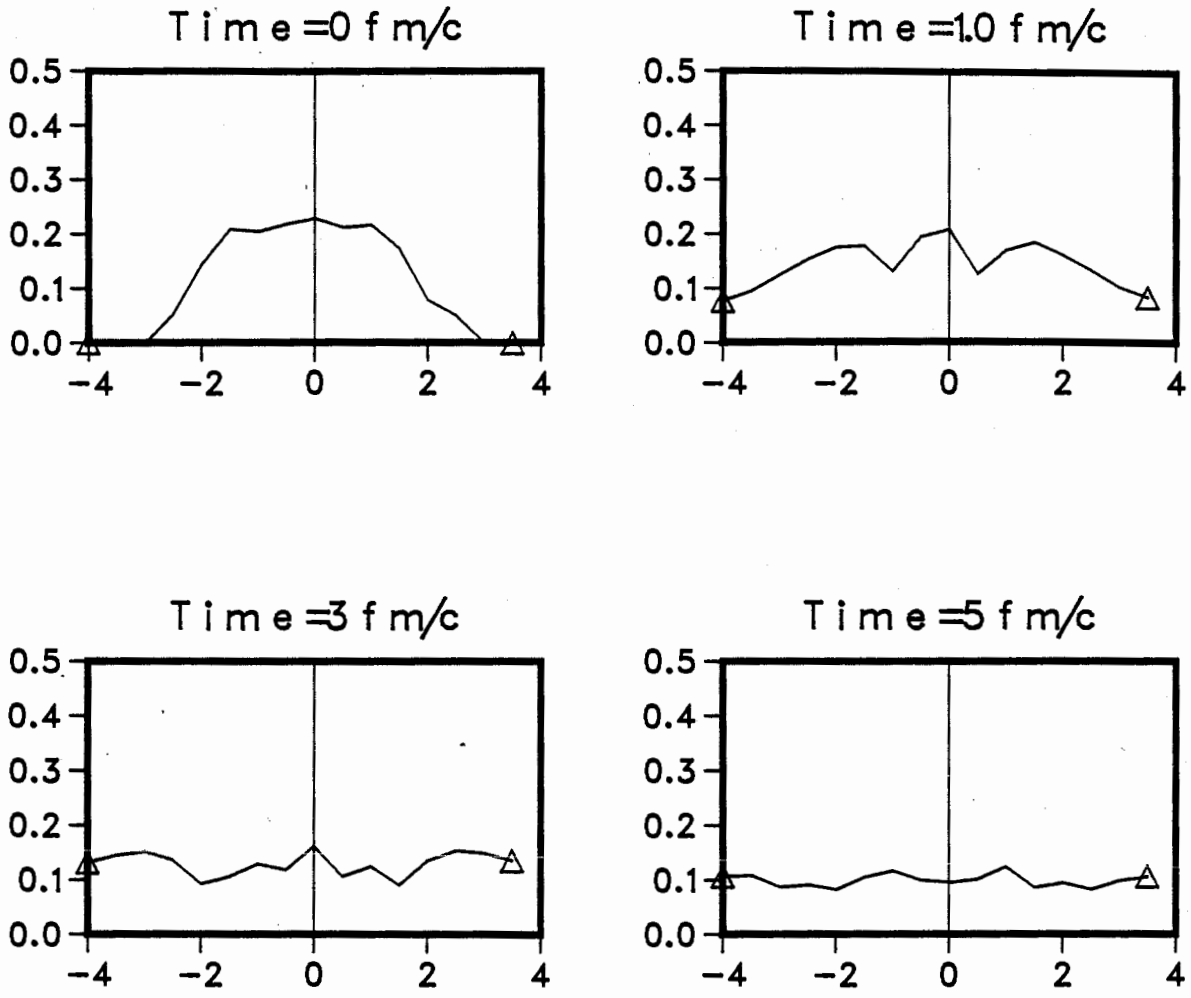

Fig. 6. The longitudinal distribution of temperature. The units of vertical axis are GeV and the units of horizontal axis are fm.

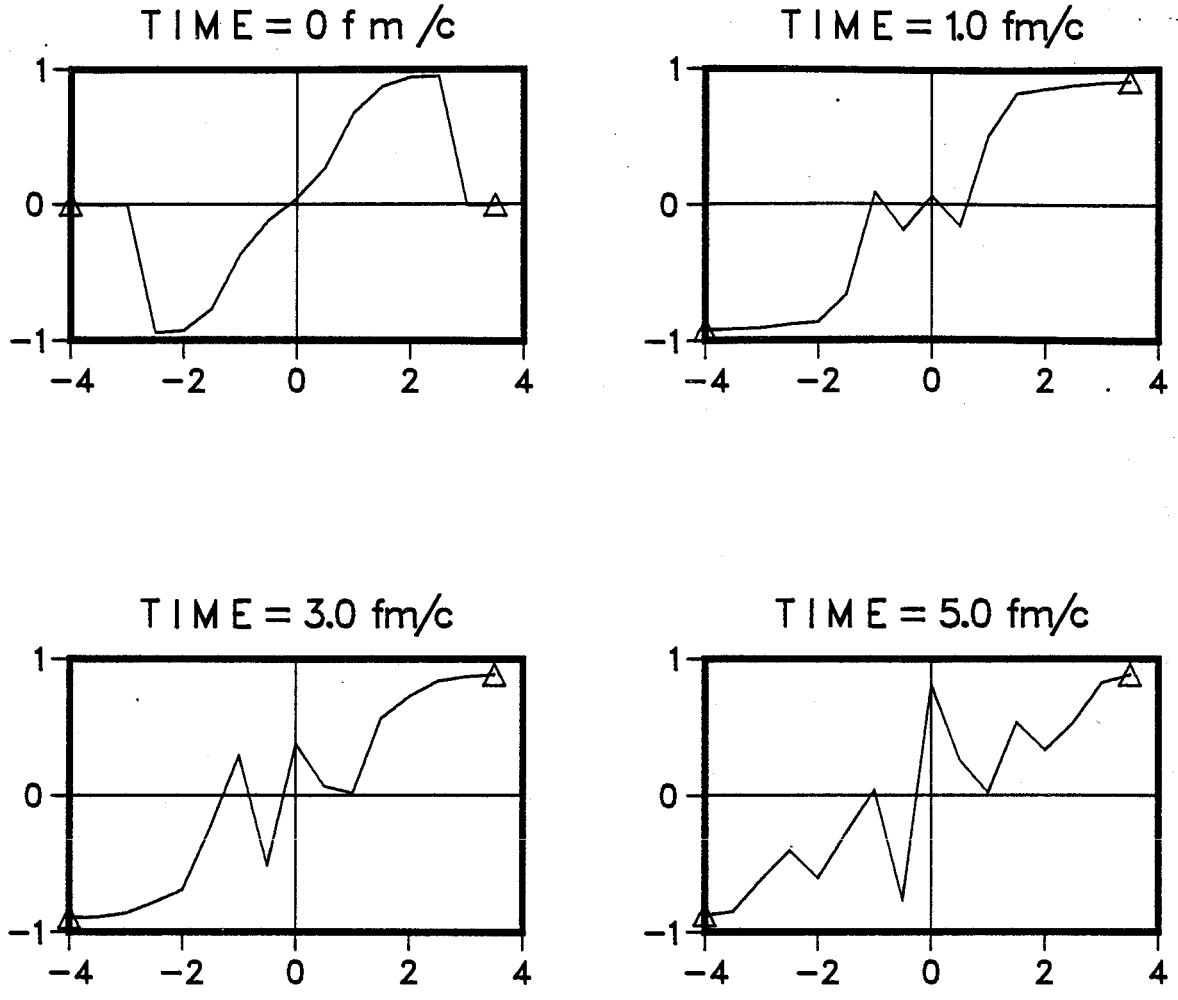

Fig. 7. The longitudinal distribution of longitudinal velocity.

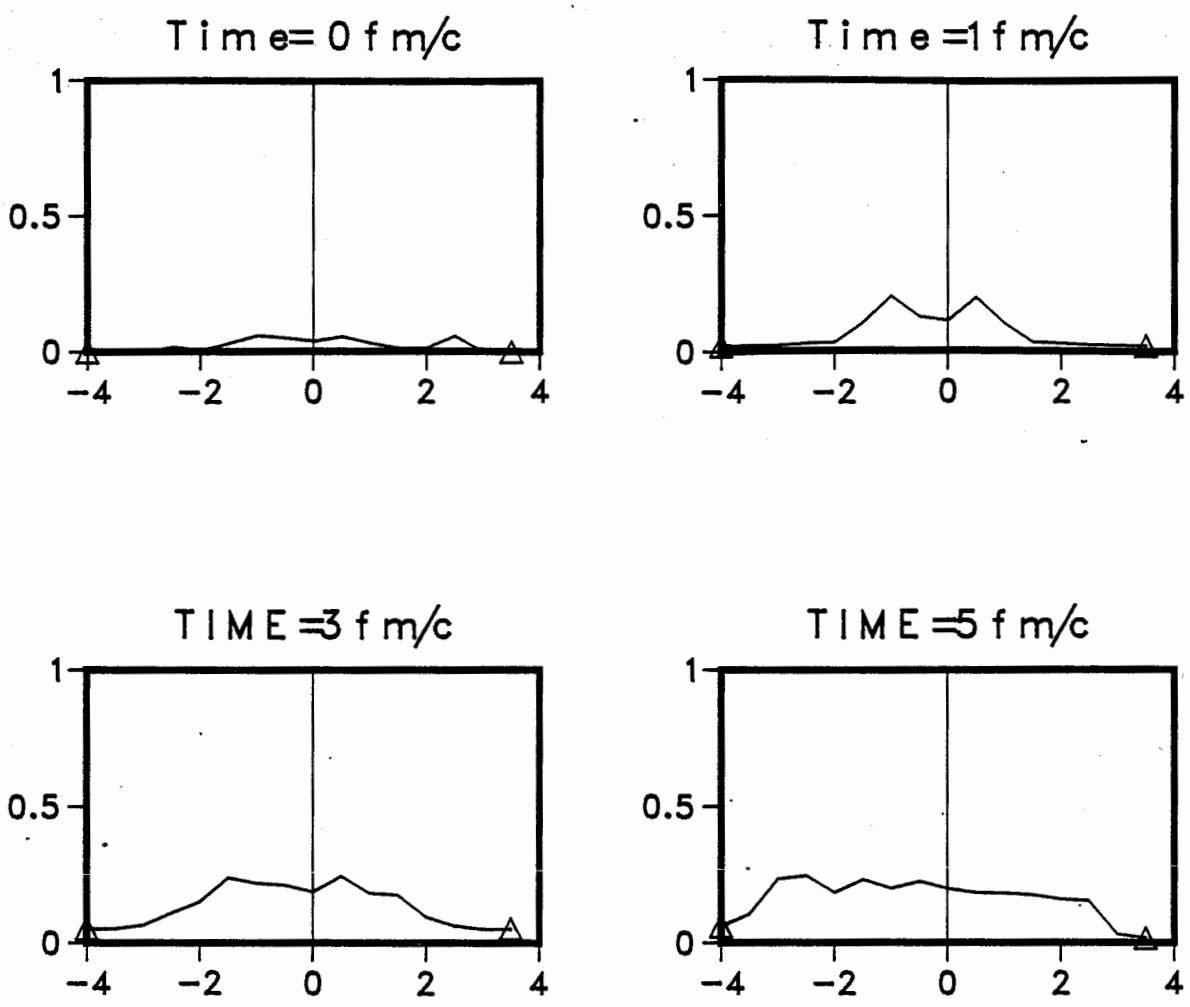

Fig. 8. The longitudinal distribution of transverse velocity.

graphs, the horizontal axis corresponds to the collision axis and the size of this axis is exactly the same as the size of longitudinal axis of the computer generated mesh. Each figure has four graphs which corresponds to different time steps. For calculating a variable at a particular point in the longitudinal direction an average is taken over transverse directions. In all the figures, the first plot corresponds to the computer generated initial conditions. In Fig. (5) where the longitudinal distribution of energy density is plotted, we see at z=0(where the longitudinal axis is labelled as z) the energy density is maximum and it falls off as we go away from z=0. With time the energy density decreases and finally at late times like t =4fm/c or t =5fm/c it is roughly zero for all the fluid cells. It means that around this time most of the fluid has expanded outside the boundaries of the computer generated mesh. Fig. (6) shows the behaviour of temperature. In Fig. (7) and Fig. (8) we have plotted the longitudinal and the transverse velocities respectively. The transverse velocity of a fluid cell is defined as, $v_t=(v_x^2 + v_y^2)^{1/2}$. For times between 0-2fm/c most of the fluid cells in the center have zero longitudinal velocity whereas the fluid cells at the boundaries are moving with a velocity close to the velocity of light. Initially, the transverse velocity of the fluid cells at the center is small compare to the longitudinal velocity but it increases with time. Similarly in Fig. (9), (10), (11) and (12) the transverse distribution of energy density, temperature, longitudinal velocity and the transverse velocity are plotted versus one of

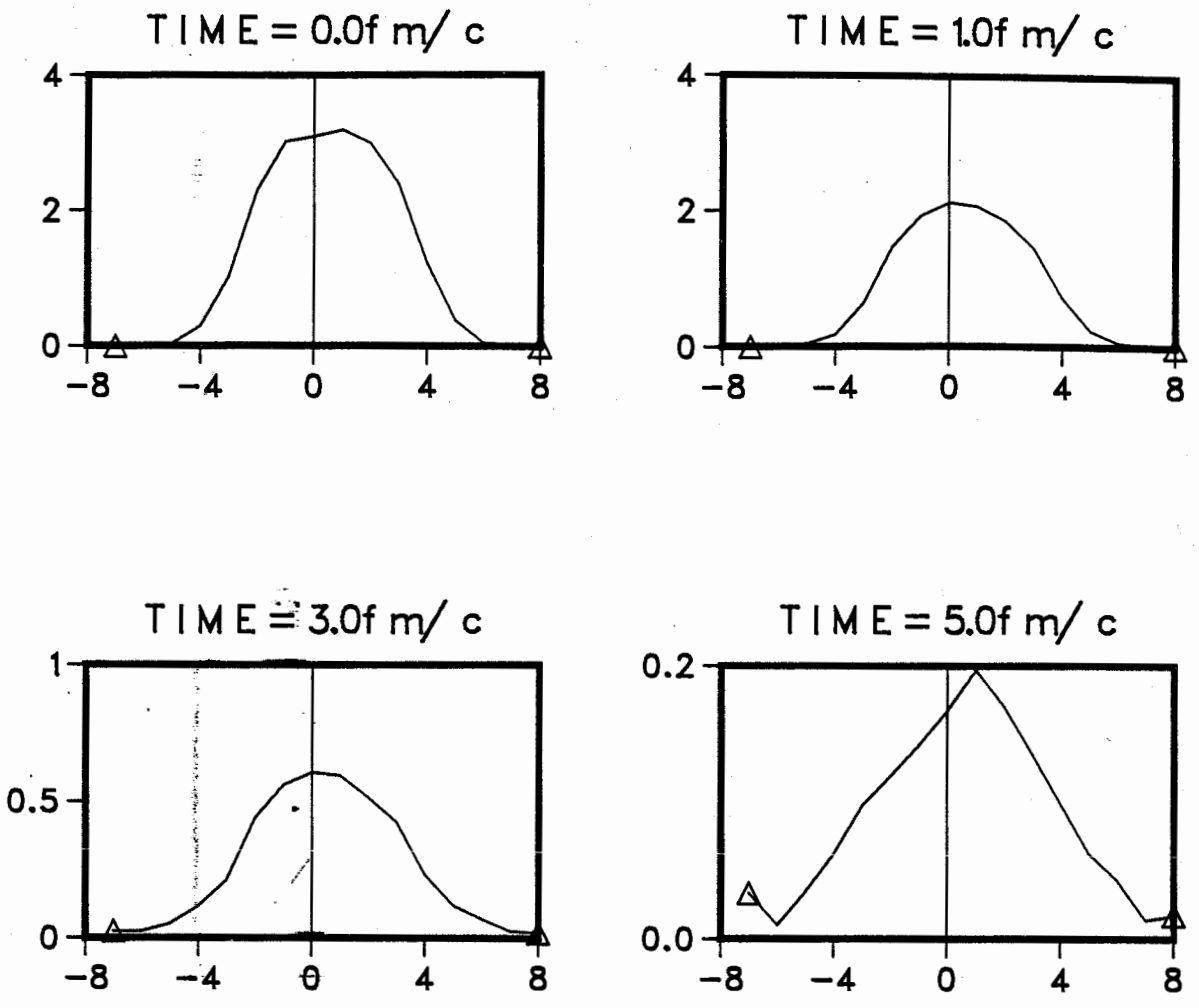

Fig. 9. The transverse distribution of energy density.

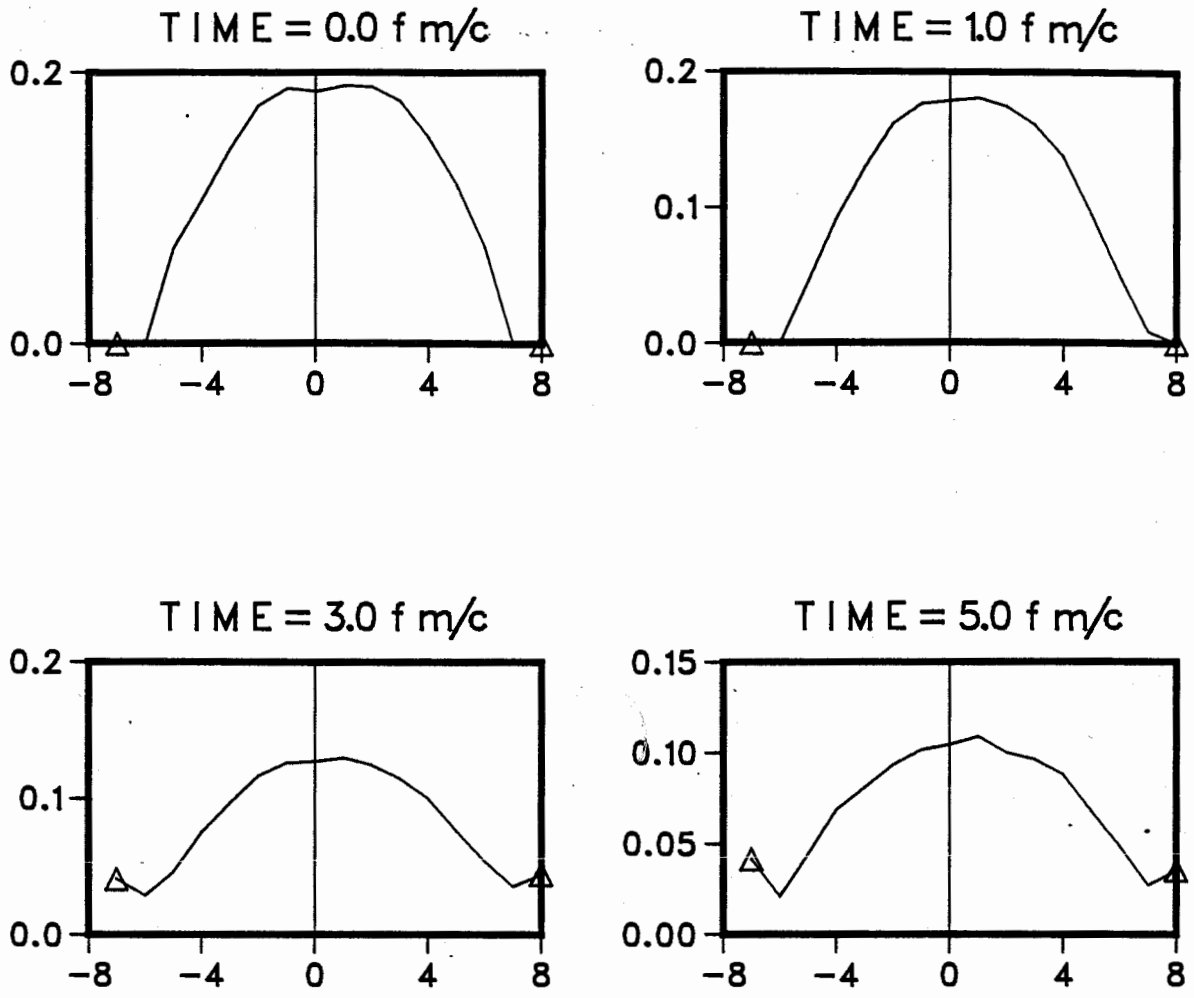

Fig. 10. The transverse distribution of temperature.

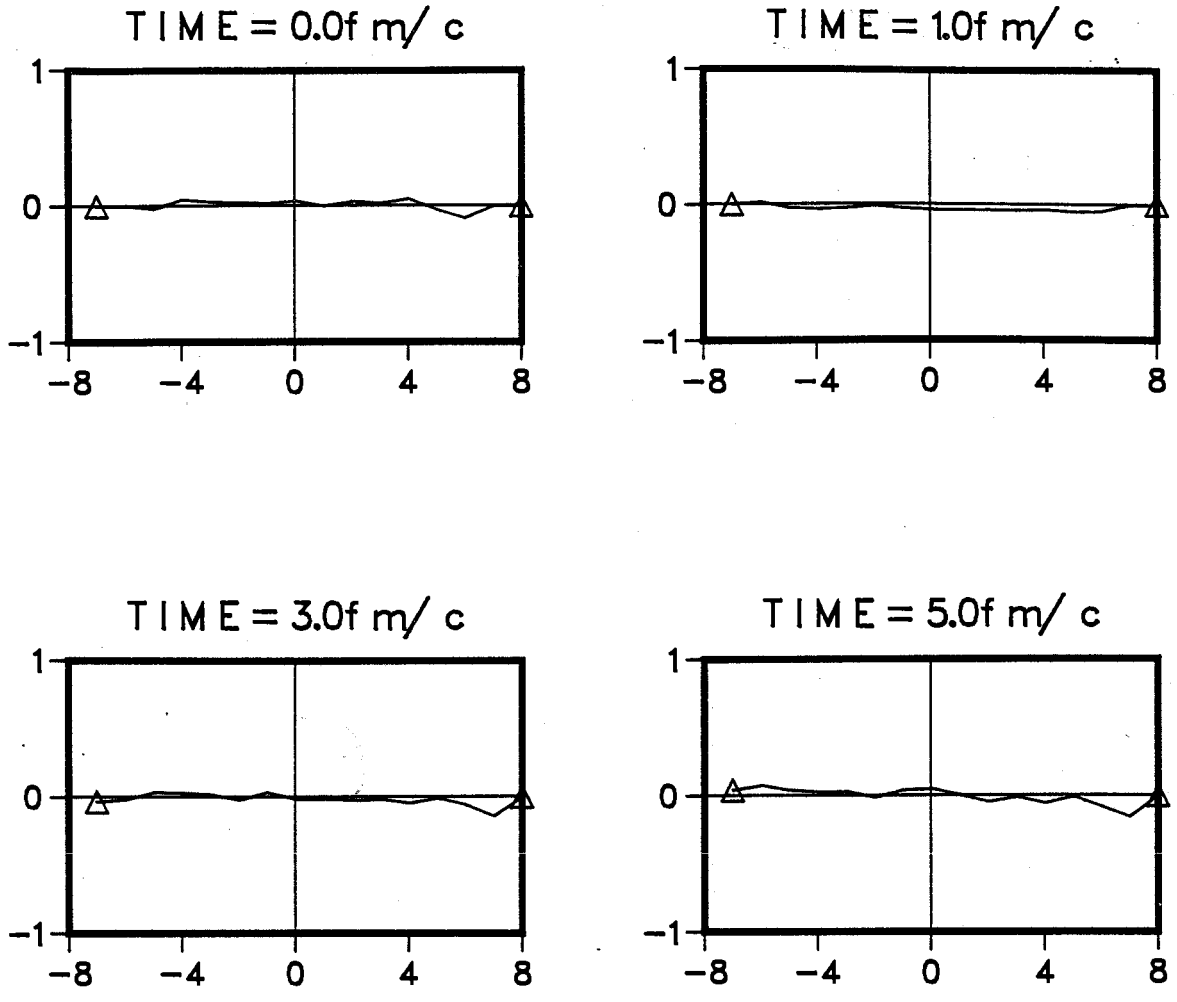

Fig. 11. The transverse distribution of longitudinal velocity.

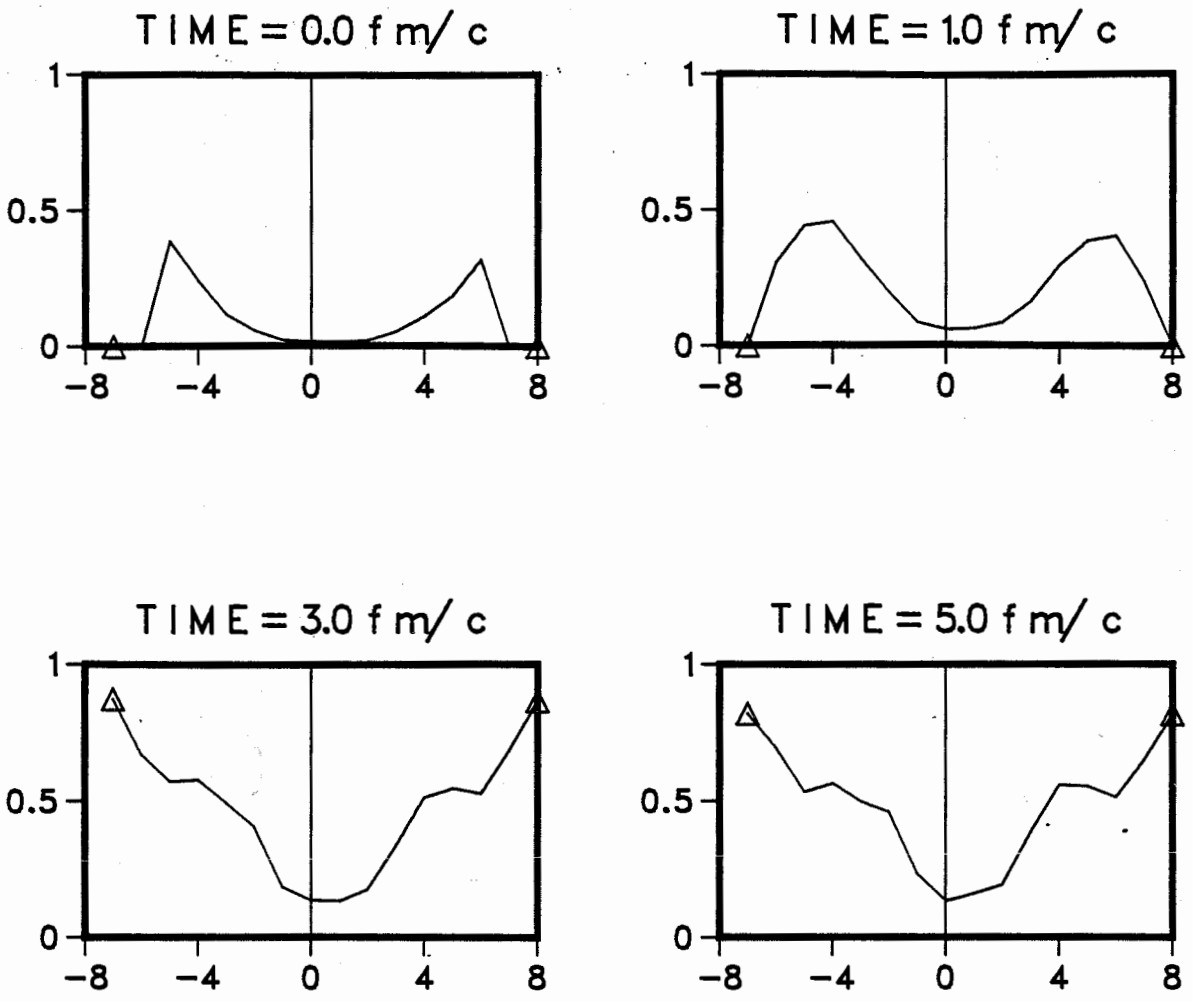

Fig. 12. The transverse distribution of transverse velocity.

the transverse direction. The value of a variable, at a particular point in the transverse direction, is calculated by taking the average over the longitudinal direction. The transverse distribution of the energy density and the temperature, shown in Fig. (9) and Fig. (10), almost looks like a normal distribution.

CHAPTER 4

EXPERIMENTAL SIGNATURES OF THE PLASMA

The quark-gluon plasma phase is very short lived i.e. the initial plasma temperature T_o will fall off very rapidly to the critical temperature T_c. This fall off is due to the volume expansion and the emission of particles from the surface of the plasma. There are number of possible scenarios that have been discussed by different authors,[25,32,65] as to how the system will go through the confinement phase transition. For example, in one scenario[25] the system at T_c will exist in a mixed phase for an appreciable length of time. In that case an equilibrium phase transition, based on the Maxwell condition for coexisting phases, occurs. In another scenario[32], the plasma supercools to some temperature T_{qg} below T_c at which point the plasma makes a sudden transition to a superheated hadron vapour at a temperature T_h above T_c. In this scenario the transition from one phase to the other is assumed to be instantaneous. Both possibilities are shown in Fig.(13). In any case, the interactions between the plasma constituents will not cease at the phase transition. The characteristic kinematical signature, if any, exhibited by the quark-gluon plasma, would almost with certainty be destroyed by these final state interactions. Therefore, any analysis which can be helpful in determining a direct or indirect signal for the plasma formation must be based upon the observables that are not affected by the final state interactions. One such observable has been discussed here in

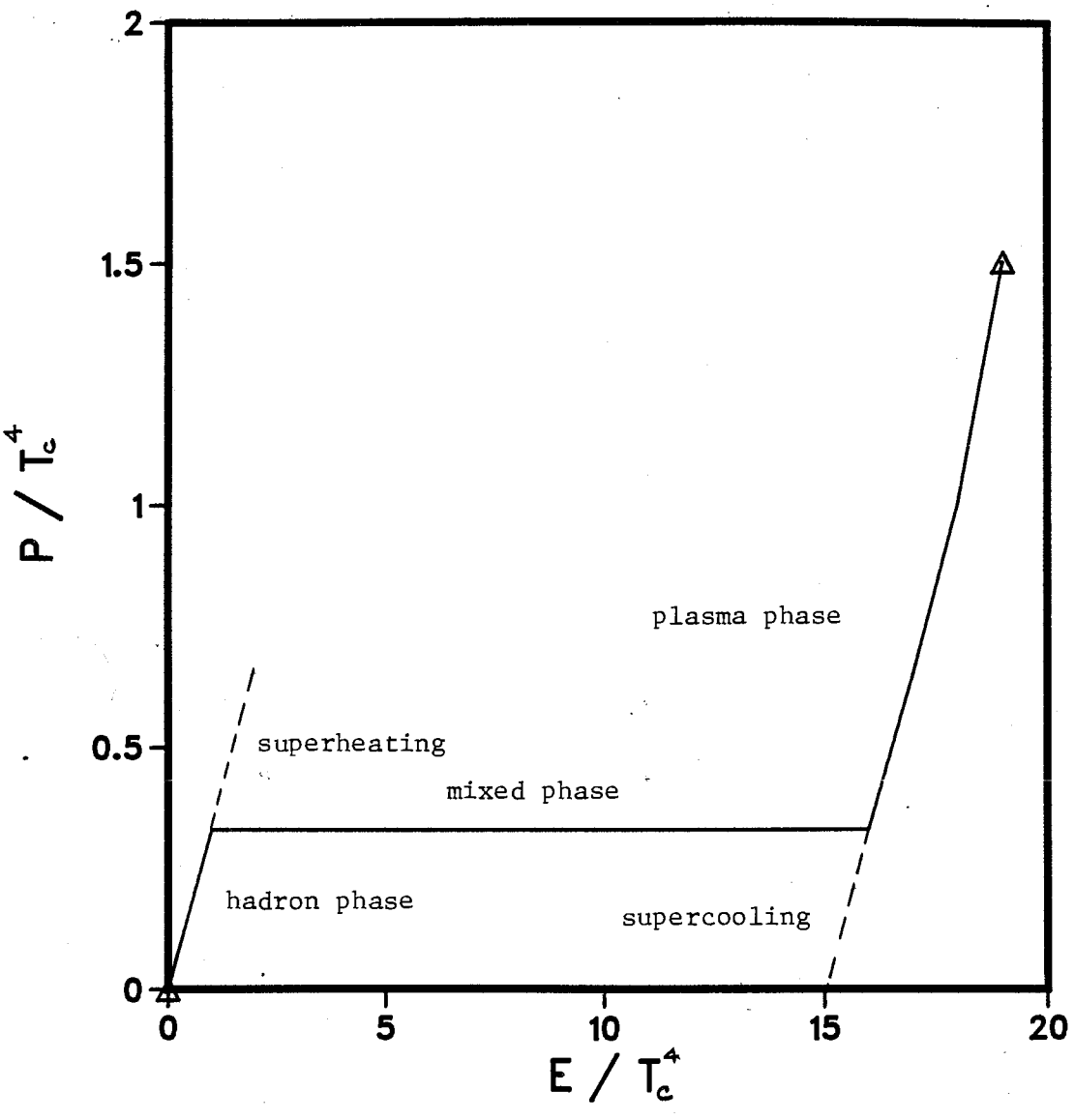

Fig. 13. The equation of state and different possible scenarios for the phase transition are shown.

detail; quantum numbers that remain unchanged by strong interactions such as strangeness or charm.

In recent years many authors[30,32,58] have considered strangeness production as the most promising signal for the formation of quark-gluon plasma. The reason for this is as follows: as the quark-gluon plasma lifetime is much too short for weak interactions to be of importance, strangeness once produced can only be destroyed if a strang quark and a strange antiquark meet and annilihate. Such a process is not very likely unless strange quarks are very abundant. Therefore, the amount of strangeness observed, long after the reaction is over, can be expected to be a good signal for the formation of quark-gluon plasma, so long as interactions in the hadronic phase do not result in appreciable strangeness production as well. In the plasma phase, it is argued that a large amount of strangeness will be produced because of the small mass of the strange quark in comparsion to the temperatures of interest.

An important question, which should be answered before one deals with the problem of strangeness production is, whether the plasma is in local chemical equilibrium or not. For a static quark-gluon plasma in chemical equilibrium, the chemical potentials μ_i and the number of particles n_i (subscripts i refer to different species) are constant with respect to time. When the plasma is not in chemical equilibrium, the question of how fast the plasma gets to the state of chemical equilibrium depends upon the relaxation time and lifetime of the plasma. The

essential ingredients required for answering this question are the production and annihilation rates of strangeness inside the plasma. Such analysis also requires the knowledge of different chemical reactions responsible for the annihilation and the production of strangeness, and also the cross sections associated with them. With the help of rates and cross sections, one can evaluate the rate equation which will determine the time evolution of strange quarks. Another added complication arises, because of final state Pauli blocking on the rate constants for the strangeness production processes. As more and more strange quarks and antiquarks are produced they occupy, in part, the available phase space and may impede production through the influence of the Pauli exclusion principle.

Therefore, in the next section, rates and cross sections are calculated for different strangeness producing reactions. A rate equation is discussed as well as some simple models which were used in the past [30,32] for studying the strangeness production as a signal for the plasma formation are discussed.

4.1 STRANGENESS PRODUCTION RATES AND CROSS SECTIONS:

In lowest order in perturbative QCD $s\bar{s}$-quark pairs can be created by annihilation of light quark-antiquark pairs and in the collision of two gluons. Feynman diagrams governing the creation of $s\bar{s}$-quark pairs are shown in Fig.(14). Diagrams (14a)-(14c) correspond to the creation of $s\bar{s}$-quark pair from gluon annihilation and diagram (14d) corresponds to the creation

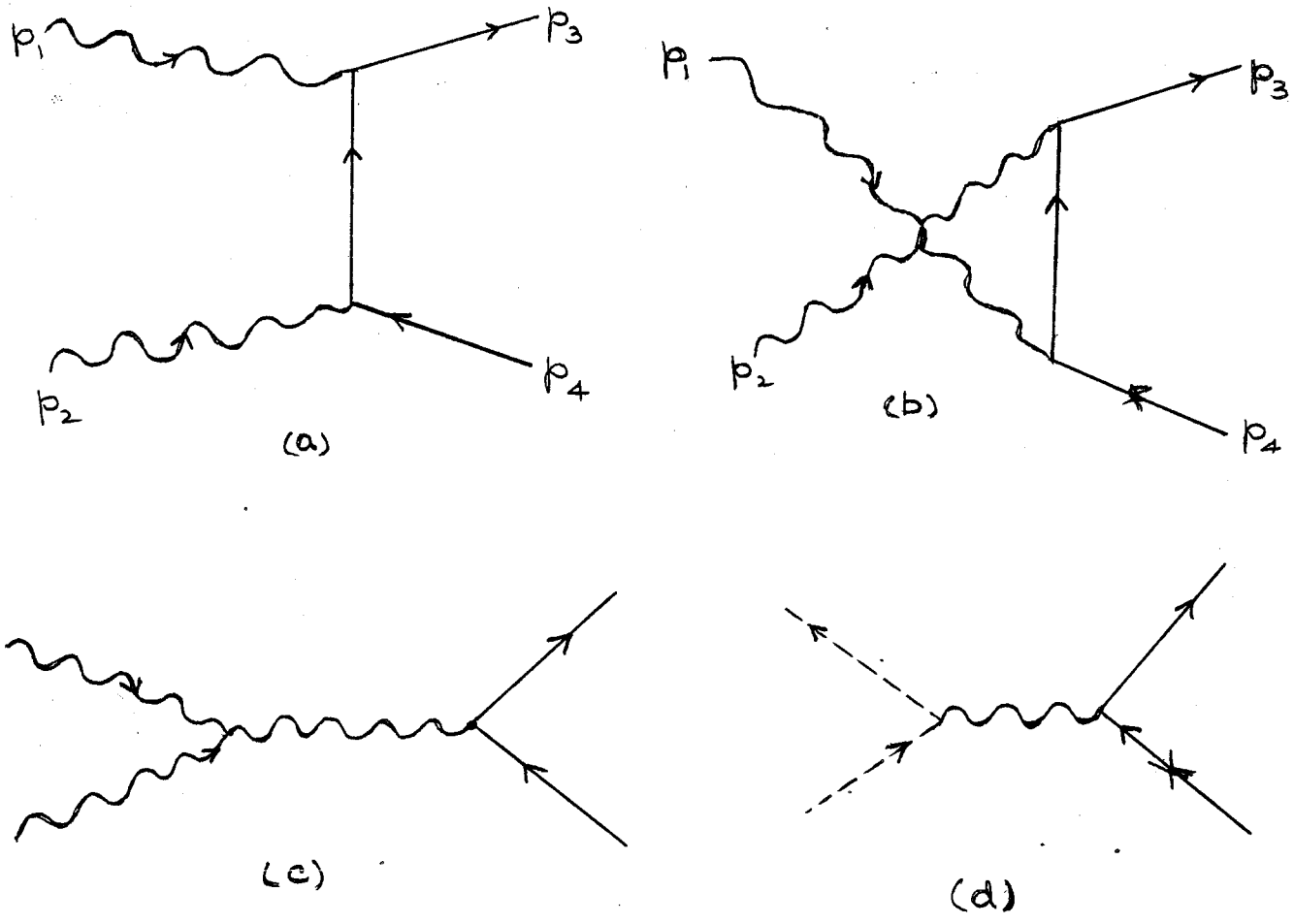

Fig. 14. The different strangeness generating processes in the lowest order of QCD in the quark-gluon plasma.

of $s\bar{s}$-quark pair from light quark annihilation. The invariant matrix elements for processes in Fig.(14) have been calculated by Georgi et.al,[59] Combridge[60] and by Matsui and McLerran.[58] The squared invariant matrix elements, summed over initial and final colour, spin and flavour states are for the individual digrams shown in Fig.(14) respectively:

$$\Sigma|\Xi_a|^2 = \gamma_g^2\ \gamma_q^2\pi^2\alpha_s^2\ \{[(m^2-t)(m^2-u)]/(3s^2)\}, \tag{4.1}$$

$$\Sigma|\Xi_b|^2 = \gamma_g^2\ \gamma_q^2\pi^2\alpha_s^2\ 2/27\{[(m^2-t)(m^2-u)-2m^2(m^2+t)]/(m^2-t)^2\}, \tag{4.2}$$

$$\Sigma|\Xi_c|^2 = \gamma_g^2\ \gamma_q^2\pi^2\alpha_s^2\ 2/27\{[(m^2-t)(m^2-u)-2m^2(m^2+u)]/(m^2-u)^2\}, \tag{4.3}$$

$$\Sigma\Xi_a\Xi_b^* = \gamma_g^2\ \gamma_q^2\pi^2\alpha_s^2\ 1/12\{[(m^2-t)(m^2-u)+m^2(u-t)]/(s(m^2-t))\}, \tag{4.4}$$

$$\Sigma\Xi_a\Xi_c^* = \gamma_g^2\ \gamma_q^2\pi^2\alpha_s^2\ 1/12\{[(m^2-t)(m^2-u)+m^2(t-u)]/(s(m^2-u))\}, \tag{4.5}$$

$$\Sigma\Xi_b\Xi_c^* = \gamma_g^2\ \gamma_q^2\pi^2\alpha_s^2\ 1/108\{[m^2(s-4m^2)]/[(m^2-u)(m^2-t)]\}, \tag{4.6}$$

$$\Sigma|\Xi_d|^2 = \gamma_q^4\ \pi^2\alpha_s^2N_f\,16/81\ [(m^2-t)^2+(m^2-u)^2+2m^2s]/s^2, \tag{4.7}$$

Here $s=(p_1+p_2)^2$, $t=(p_3-p_1)^2$, and $u=(p_3-p_2)^2$, which satisfy $s+t+u = 2m^2$, are the Mandelstam variables. The four momenta of the incoming particles are p_1 and p_2 while p_3 and p_4 are the four momenta of outgoing particles and m is the mass of strange quark. The number of light quark flavours contributing to the reaction $q\bar{q}$-$s\bar{s}$ is N_f =2. The degeneracy factors for gluons and

quarks are:

$$\gamma_g = 2_s 8_c = 16, \quad \gamma_q = 2_s 3_c = 6.$$

The strong coupling constant α_s taken here at an invariant momentum Q^2 which is chosen as $Q^2 = s$.[60] As this choice for Q^2 is independent of the squared momentum transfer t, the averaged cross sections may be easily determined by integrating over the allowed range of t:

$$\bar{\sigma} = 1/(16\pi s^2) \int_{t_-}^{t_+} dt \; \Sigma |\Xi|^2, \tag{4.8}$$

where $t_+ = m^2 - (s/2)(1-W(s))$, $t_- = m^2 - (s/2)(1+W(s))$ and $W(s) = (1-4m^2/s)^{1/2}$. Thus one finds:

$$\bar{\sigma}_{qq-ss} = 8\pi\alpha_s^2/(27s)(1+2m^2/s)W(s), \tag{4.9}$$

$$\bar{\sigma}_{gg-ss} = 2\pi\alpha_s^2/(3s)\{[1+4m^2/s+m^4/s^2] \tanh^{-1}W(s) - [7/8+(31/8)m^2/s]W(s)\}. \tag{4.10}$$

The rate R, which is a function of temperature, is defined to be the number of reactions of the specified kind per unit volume per unit time. For a reaction of the type a+b→c+d, the principal physics is contained in the factor $\langle\sigma(a+b\to c+d)v_{rel}\rangle$, where v_{rel} is the relative velocity of a and b defined as $p_1 \cdot p_2/|p_1||p_2|$, and the angular brackets denote an averaging over relative velocities of a and b. The invariant rate per unit time per unit volume for the elementary processes shown in Fig.(14) is then[58]

$$R=dN/dtd^3x=1/2\int_{4m^2}^{\infty}sds\delta(s-(p_1+p_2)^2)\int d^3p_1/\ [(2\pi)^3|p_1|]$$
$$\int d^3p_2/(2\pi)^3|p_2|\ [1/2\gamma^2_g f_g(p_1)f_g(p_2)\ \bar{\sigma}_{gg-ss}(s)+$$
$$N_f\ \gamma^2_q f_q(p_1)f_q(p_2)\ \bar{\sigma}_{qq-ss}(s)]. \qquad (4.11)$$

The factor 1/2 in front of the phase space density of gluons accounts for the fact that the double integration over p_1 and p_2 counts each gluon pair twice.[58] In the above equation $f_g(p_i)$ and $f_q(p_i)$ are the momentum distribution functions. These functions are approximated by the Bose and Fermi distribution functions respectively:

$$f_g(p;x) =1/\{\exp[\beta_\mu(x)p^\mu] -1\}$$
$$f_q(p;x) =1/\{\exp[\beta_\mu(x)p^\mu] +1\}, \qquad (4.12)$$

where for light quarks and gluons $p^2=0$ and for strange quarks $p^2=m^2$. For the gluonic part of R, the integrals over p_1 and p_2 can be carried out analytically by expanding the Bose function in a power series in exp(-p/T) and putting this in equation (4.11);

$$R_g \simeq 7/(6\pi^2)\alpha_s^2\ mT^3\exp(-2m/T)(1+51/14\ T/m+----). \qquad (4.13)$$

For calculating the quark contribution to the reaction rate, the integrals must be evaluated numerically. The rates have been computed numerically and plotted in ref.30 for $0.43 \leq m/T \leq 2.0$. Another parametrization in that range suggested by J. Kapusta

and A. Mekjian[32] is

$$R(gg \text{ or } qq\text{-}ss) = 2\alpha_s^2 T^4 \exp(-2m/T). \qquad (4.14)$$

For $\alpha_s = 0.4$ and $m = 180MeV$, the plot of R versus T using equation (4.14) is shown in Fig.(15).

For calculating the relaxation time, consider a static quark-gluon plasma. It means all thermodynamic variables depend on time and are uniform in space. What is needed here is a rate equation which can take into account both the annihilation and production of strange quarks. If the statistical independence of the production and annihilation processes is assumed then the loss term is proportional to the square of the density n_s of strange and antistrange quarks at a particular time.[30] Then the following differential equation describes the time evolution of n_s:

$$dn_s/dt = R[1-(n_s(t)/n^{eq.}_s)^2], \qquad (4.15)$$

where $n^{eq.}_s$ is the equilibrium density of strange at a particular temperature. For fixed temperature, the solution to (4.15) is

$$n_s(t) = n^{eq.}_s \tanh[t/(2\tau + \text{const.}], \qquad (4.16)$$

where τ is the relaxation time given by

$$\tau = n^{eq.}_s/(2R). \qquad (4.17)$$

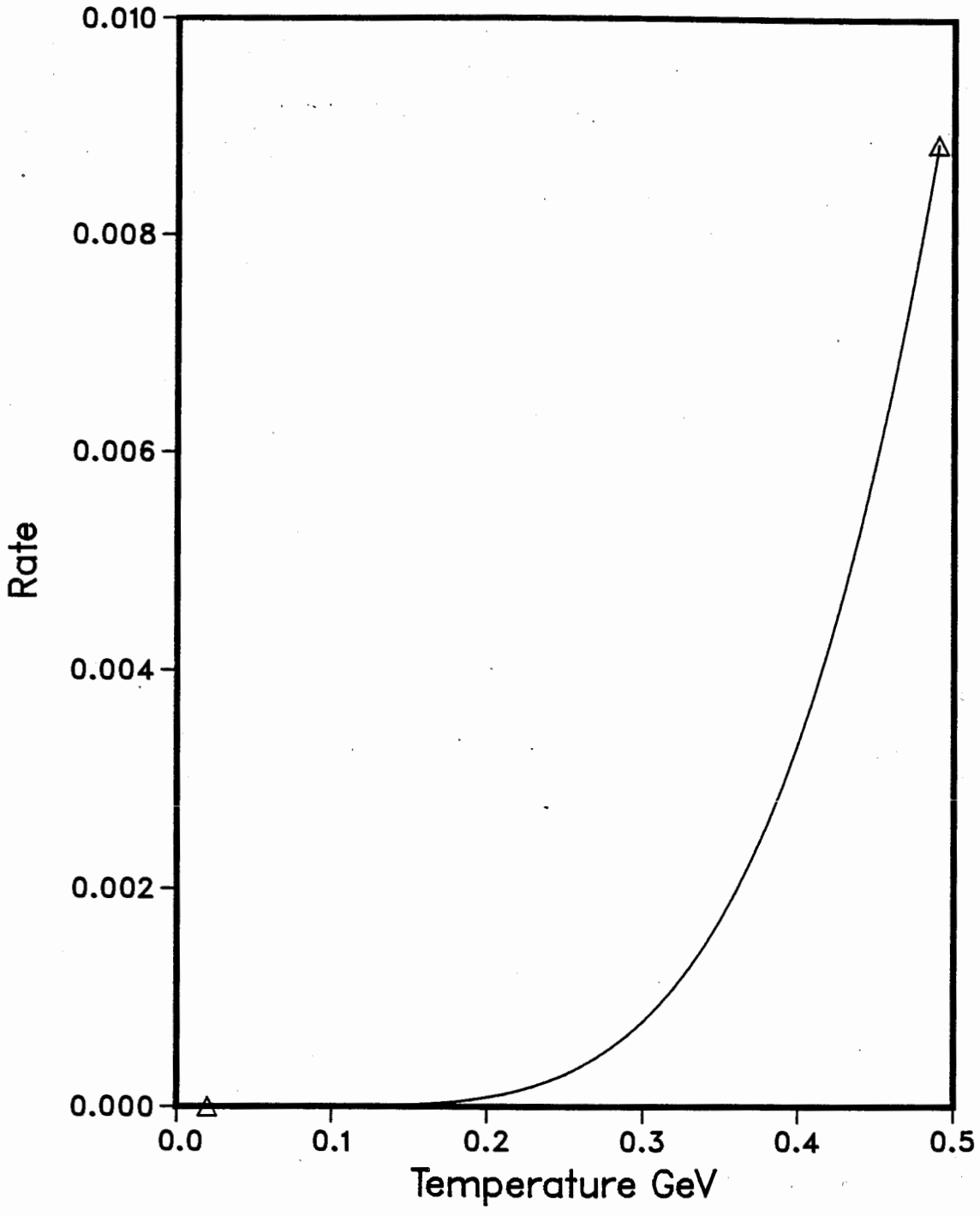

Fig.15. The plot of production rate for strange quarks in the plasma phase, mass of the strange quark is taken to be 0.180GeV and the strong coupling constant is 0.4.

The s-quark equilibrium number density is

$$n^{eq.}_s = 6\int d^3k(2\pi)^{-3}\ \{\exp[(k^2+m^2)^{1/2}/T]+1\}^{-1}. \qquad (4.18)$$

For an expanding plasma, where all thermodynamic variables depend on time and space variables, a dilution term must be included in equation (4.15) to account for the change in volume with respect to time. In this case one can write

$$dn_s/dt = R[1-(n_s(t)/n^{eq.}_s)^2]-n_s(t)/V\ dV/dt. \qquad (4.18)$$

Equations (4.14-4.18) will be used later, when a model used by J. Kapusta and A. Mekjian is discussed.

4.1.1 KAON TO PION RATIO:

A proposed signal for the formation of the quark-gluon plasma is the relative abundance of kaons to pions. This can be explained as follows for a baryon-free plasma: at a fixed temperature T the density of non-interacting strange quarks is much higher than the density of non-interacting kaon, because of the following two reasons.

(a) Strange quarks have more degrees of freedom (two spin and three colour) than the kaons.

(b) The current mass of a strange quark (roughly, m=180MeV) is less than the mass of kaon (m_K=494MeV). This gives a much greater suppression through the Boltzmann factor for kaons than for the strange quarks.

For calculating the kaons to pions ratio, authors of ref.(32)

have used a thirty-year-old idea due originally to Landau.[61] According to this idea, the measure of strangeness content is the strangeness density divided by the entropy density, which is a dimensionless number. Ref. 32 has taken simple Bjorken's model for longitudinal hydrodynamic expansion of the plasma. Most important of all, the entropy density in this model is determined as function of time through the following differential equation,

$$ds/dt = -s/t \text{ or } s(t) = (t_0/t)s_0. \qquad (4.19)$$

For determining the temperature as function of time, the following expression for the entropy density in the plasma phase is being used,[32]

$$s_{qg} = (74/45)\pi^2 T^3. \qquad (4.20)$$

Here only two flavours of quarks(up and down) are taken and they are assumed to be massless and the chemical potential of the plasma is taken to be zero. From eq.(4.19) and (4.20), one can find out the time development of temperature i.e.

$$T(t) = T_0(t_0/t)^{1/3}, \qquad (4.21)$$

where T_0 is the initial temperature of the plasma. In this scenario, initially the system is completely in the quark-gluon plasma phase. By time t_1, temperature has dropped to the critical temperature T_c and from then on system is assumed to be

in mixed phase i.e. consisting of quark-gluon plasma and hadrons. During this adiabatic phase transition the system stays at T_c until all the latent heat is converted to expansion energy. The time t_1 when the system first enters the mixed phase, can be obtained from eq.(4.21),

$$t_1 = (T_0/T_c)^3 t_0. \tag{4.22}$$

For calculating the entropy density in the mixed phase, let us denote f(t) as the volume fraction of matter which is in the plasma phase. Then

$$s(t) = f(t)s_{qg}(T_c) + [1-f(t)]s_h(T_c) , \tag{4.23}$$

where $s_h(T)$ i.e. the entropy density in the hadronic phase. For a hadronic gas consisting of massless pions, it is given by the following equation,

$$s_h = (2\pi^2/15)T^3. \tag{4.24}$$

The change in the entropy density is due to the volume expansion of the system. By combining eq.(4.23) and (4.19), one can solve for f(t) i.e.

$$f(t) = (37/34)(T_0/T_c)^3 t_0/t - 3/34. \tag{4.25}$$

The time t_2 at which the phase transition is completed, can be obtained with the help of condition that $f(t_2) = 0$,

$$t_2 = (37/3)t_1. \qquad (4.26)$$

For tracking the time evolution of strangeness density the rate eq.(4.18) is being used. For one dimensional longitudinal expansion where $V \sim 1/t$, eq.(4.18) gives

$$dn_s(t)/dt = R_{qg}[1-(n_s(t)/n^{eq.}_s)^2]-n_s(t)/t, \qquad (4.27)$$

where R_{qg} is obtained by using eq.(4.14). The initial condition is chosen to be $n_s(t_0) = 0$. In the mixed phase, the rate equation for kaons is

$$dn_K/dt = R_h(T_c)[1-(n_K(t)/n^{eq.}_K)^2]-n_K(t)/(f'(t)t)$$
$$d[f'(t)t]/dt+(1/2)n_s(t)/f'(t)df'(t)/dt. \qquad (4.28)$$

Here $f'(t) = 1-f(t)$ is the fraction of the system which is in the hadron phase. The rate of strangeness production for the hadronic phase is [62]

$$R_h = 2(R_A+R_B)$$
$$R_A = AT^6/(8\pi^4)z_0^3K_3(z_0)$$
$$R_B = BT^6/(64\pi^3)z_0\ (3+3z_0+z_0^2)\exp(-z_0)$$
$$z_0 = 2m_K/T,\ A = 17mb,\ B = 16mb, \qquad (4.29)$$

where m_K is the mass of a kaon and K_3 is the modified Bessel function of order 3. The equilibrium number densities for strange quarks, pions and kaons used here, are obtained as follows;

$$n_s = 6\int d^3k/(2\pi)^3 \{\exp[(m^2+k^2)^{1/2}/T]+1\}^{-1}$$
$$\simeq (3/\pi^2)m^2TK_2(m/T), \quad (4.30)$$
$$n_\pi = \int d^3k/(2\pi)^3 \{\exp[(k^2+m_\pi^2)^{1/2}/T]-1\}^{-1}$$
$$\simeq 0.1218\ T^3, \text{ (if } m_\pi = 0), \quad (4.31)$$
$$n_K = \int d^3k/(2\pi)^3 \{\exp[(k^2+m_K^2)^{1/2}/T]-1\}^{-1}$$
$$\simeq 1/(2\pi^2)m_K^2\ T\ K_2(m_K/T). \quad (4.32)$$

where m_π is the mass of pion which is 138MeV and K_2 is the modified Bessel function of second order. The integrals in eq.(4.30) and (4.32) are performed by taking the Maxwell-Boltzmann limit, whereas the integral in eq.(4.31) is performed by taking the non-relativistic limit. The initial condition for eq.(4.28) is $n_K(t_1) = 0$. Ratio of the strangeness density to the entropy density in the mixed phase is calculated as follows:

$$n_s/s = [f(t)n_s(t)+2f'(t)n_K(t)]/$$
$$[f(t)s_{qg}(t)+f'(t)s_h(t)]. \quad (4.33)$$

The behaviour of the ratio n_s/s is plotted versus time in Fig.(16), for two different values of initial temperature i.e. T_0 =250MeV and T_0 =500MeV. This ratio is a continuous function of the time, because the transition from one phase to other is continuous. For T_0 =250MeV, n_s/s ratio becomes constant around t =35fm/c and takes a saturation value which is roughly equal to 0.035. The corresponding K^-/π^- can be obtained multiplying n_s/s ratio by 5.4 (see eq.(4.31) and eq.(4.24)), and for this ratio

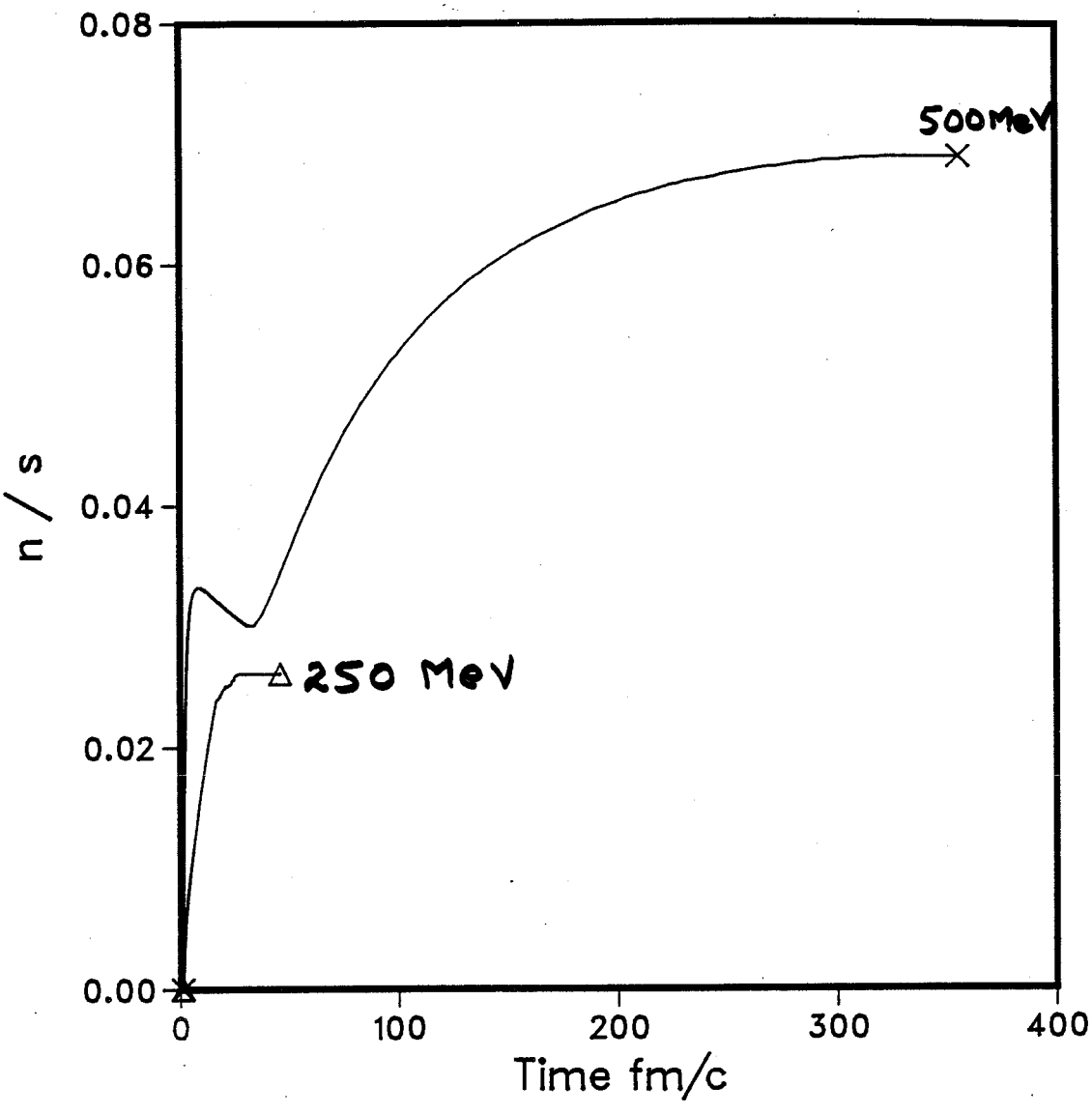

Fig. 16. The plot of the ratio of strangeness density to entropy density for two different values of initial temperature. This ratio is calculated by using the model of reference 32.

one gets 0.217. For the initial temperature of 500MeV, n_s/s ratio becomes constant around t =300fm/c and takes a saturation value which is equal to 0.055. The corresponding K^-/π^- ratio is 0.297. The observed value of this ratio at the same energy, E =10-100GeV, for $p\bar{p}$ collisions is 0.07 ± 0.02.[63] It is fair to compare with $p\bar{p}$ collisions because they form a net baryon number equal to zero system. In this model the final ratio of K^-/π^- for the quark-gluon plasma is enhanced over that in $p\bar{p}$ collisions by a factor of about 3. An independent analysis of strangeness has been carried out simultaneously by T. Matsui, B. Sevtitsky, and L. McLerran[58] with similar conclusions.

4.1.2 **THE MODEL:**

For calculating the ratio of strangeness to entropy, we have taken a different approach than in reference 32. There are number of reasons for doing this and they are given below:

(1) The most important assumption of the model used by Kapusta et.al is the validity of one-dimensional scaling hydrodynamics. In this model the tranverse expansion of the system is neglected. This implies that the entropy density $s(t) \alpha t^{-1}$ and the volume $V(t) \alpha t$. Therefore, this simple one-dimensional model gives a more slowly expanding system than what one would for a full three-dimensional model.

(2) In their model, when the system is in the mixed phase, the rate at which strangeness is fed from the plasma into the hadron phase is subject to some uncertainty. In one calculation[32] the loss term was taken to be $n_s df/dt$, so that equation (4.27) was

used at T_c instead of equation (4.15). In another calculation it was assumed that strange quarks and kaons were in chemical equilibrium.[58]

(3) The equilibrium densities for strange quarks and kaons are needed in the rate equations, which were calculated by using the Maxwell-Boltzmann limit. Therefore, this introduces another approximation in their model.

In our model, the time evolution of strange quarks is governed by the following rate equation;

$$dN_s^i/dt = V^i(t)R^i(T) \ , \qquad (4.34)$$

where N_s^i is the total number of strange quarks at some time t in a cell i with volume V^i. The production rate R for the strange quarks is taken from equation (4.14). In our model, first problem mentioned above has been cured by using full three dimensional treatment in the propagation code. This code gives ϵ, P and $\bar{v}$, at each time step, for each individual cell. The cell temperature has been calculated in the code by using the following expression,

$$T = [(30\epsilon/\pi^2)1/(16+21/2\ N_f)]^{1/4} \ . \qquad (4.35)$$

The volume of a moving cell is $V(t) = \gamma V_0$, where V_0 is the volume of the cell in the local rest frame. Using equation (4.35) in equation (4.14) one obtains the production rate, which has been

used in equation (4.34), for calculating the number of strange quarks in a cell. The total number of strange quarks in the system is obtained by summing over all the cells.

Note, in equation (4.34) we have dropped the annihilation term for the strange quarks and this takes care of the second problem. Dropping the annihilation term may slightly overestimate the number of strange quarks in the system, but even then the number of strange quarks obtained by us is smaller than the number of strange quarks obtained by other authors [30,32,58]. This also avoids the third problem because, the equilibrium densities of strange quarks and kaons are no longer needed.

In our code, by $t \simeq 3.0$fm/c, the system has expanded to the boundaries of computer generated mesh. At this point particles started to escape from the surface and because of that the total entropy and the energy of the system started to decrease. In principle, the entropy should be constant but in here it is not because of the small size of the mesh. This may possibly be achieved by taking a large space grid, but this requires much more computer memory, storage space and will slow the code down considerably. On the other hand, constant increase of the entropy in a numerical scheme implies that the numerical method used is unstable.[64] Therefore, the decrease in entropy is another check on the stability of the numerical used here. But this decreasing entropy causes a problem in the code i.e. we get a constantly increasing ratio of the strangeness to the entropy.

To cure the problem, instead of using the entropy at a particular time step we take an average over first thirty time steps. The reason for taking the average over first thirty time steps is that it corresponds to t $\simeq$ 3.0fm/c for a time step of size 0.1fm/c.

4.2 **RESULTS:**

Here we have shown two plots; the ratio of the strange quarks to the entropy versus time in Fig. (17) and the of the total number strange quarks versus time in Fig. (18). The ratio of the number of strange quarks to the entropy approaches a saturation value with respect to time and the number we obtained here for the saturation value of this ratio is 0.01. It is roughly equal to the ratio obtained from $p\bar{p}$ experiments.[67] Therefore, in our model we see no enhancement of this ratio over the ratio obtained in $p\bar{p}$ experiments. The reason for this is that in our model the plasma is expanding much faster than in the model used by refernce 32. In reference 32 the effect of the transverse expansion of the plasma is neglected resulting in a slow expansion of the plasma. Hence, the variables such as energy density and temperature decrease slowly with time and there is more time available for strangeness production. The production rate for the strange quarks in the plasma phase is proportional to the fourth power of the temperature. Therefore, if the temperature falls off rapidly with time, the production rate will fall off much faster with time. Therefore, the ratio of the

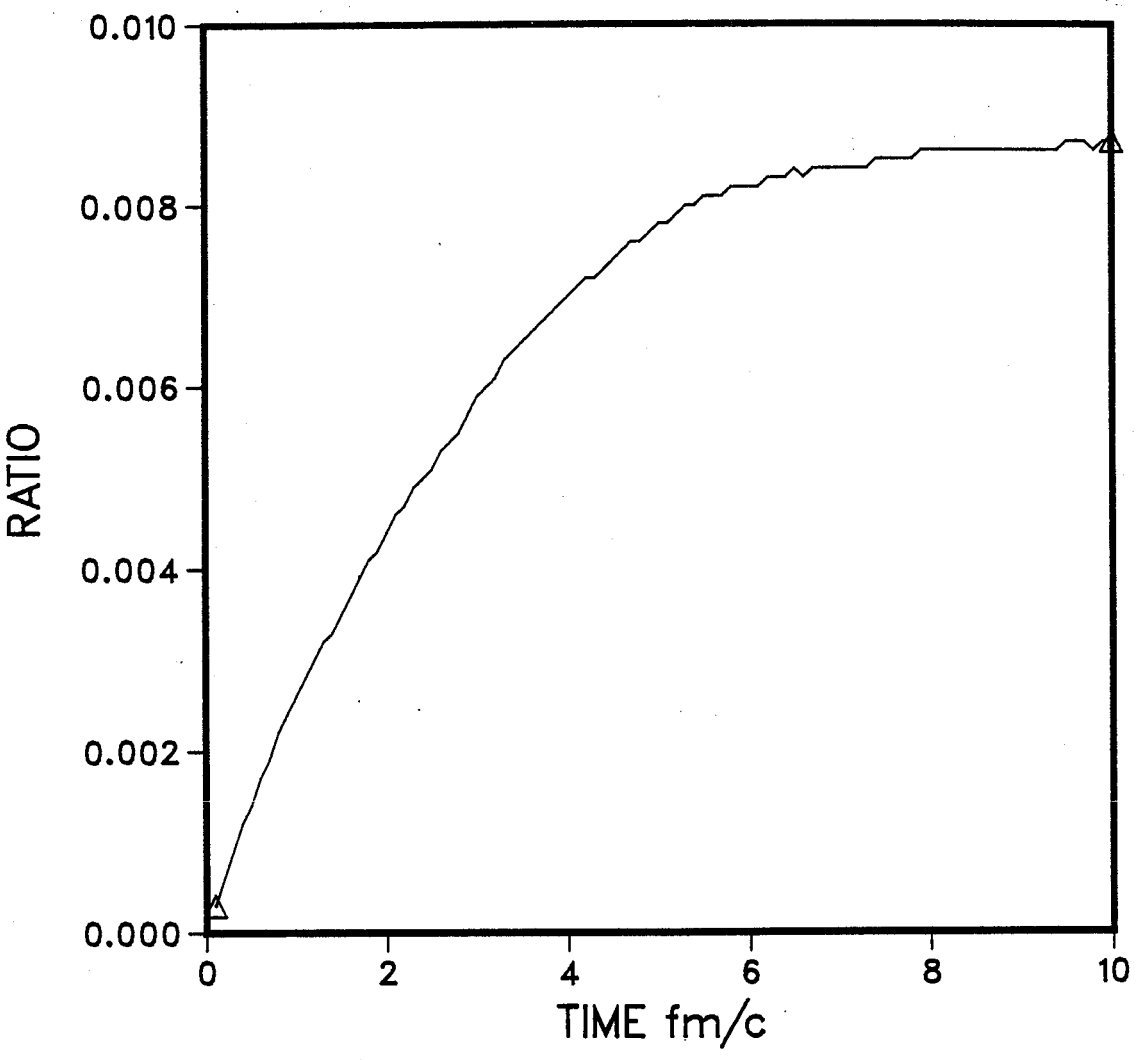

Fig. 17. The ratio of the total number of strange quarks in the plasma to the entropy of the plasma obtained by the computer simulation.

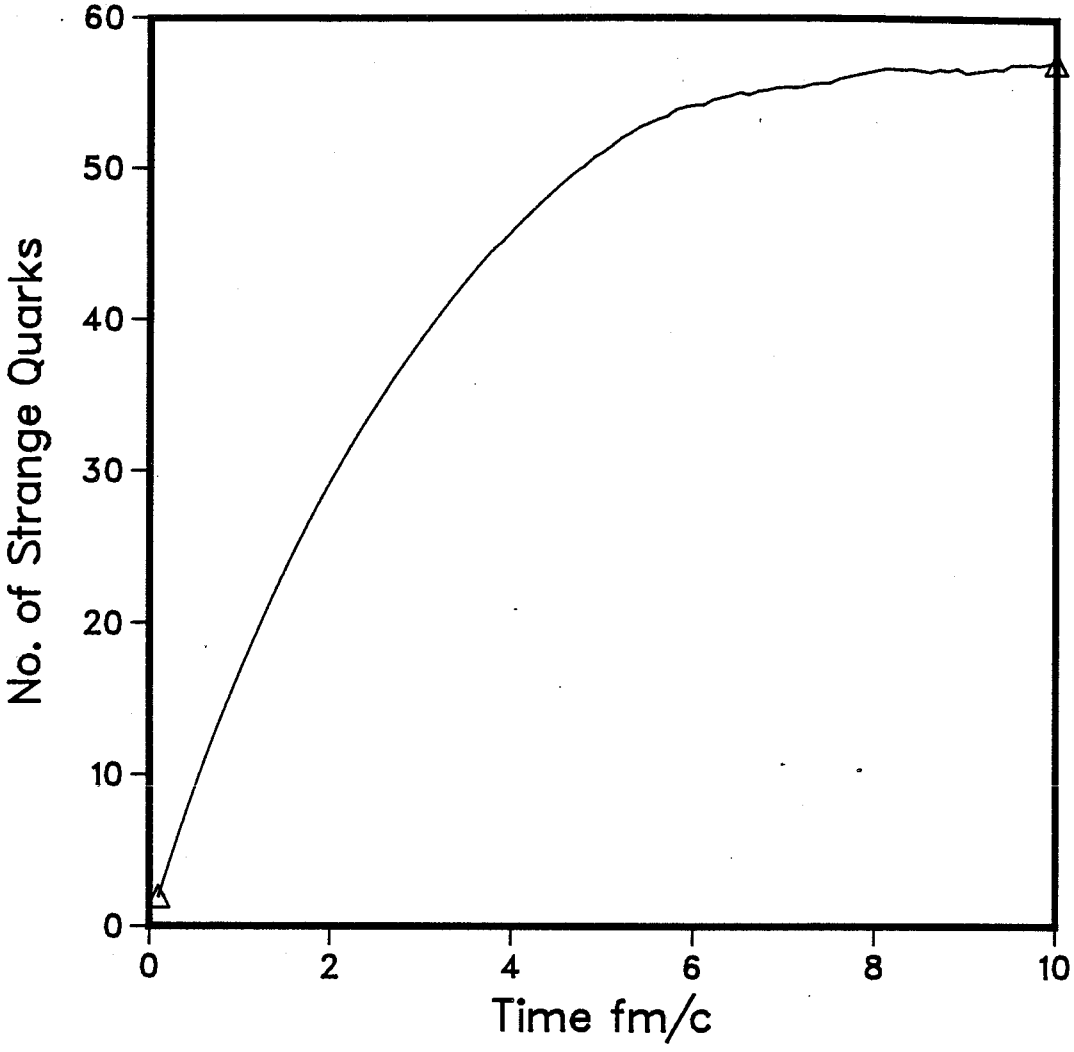

Fig.18. The plot of total number of strange quarks versus time. The total number of strange quarks is obtained from numerical simulation.

total number of strange quarks to the entropy is small in the computer simulation than the ratio obtained in reference 32. On this basis our claim is that the ratio of the total number of strange quarks to the entropy can not serve as the experimental signature for the formation of quark-gluon plasma. At least this can be said with certainty for the medium mass nuclei, because this result is obtained for a nucleus with A =50. The results might look different for the heavy nuclei such as Pb or U.

CHAPTER 5

CONCLUSIONS

Evidently many important questions have not been addressed in this thesis. The dissipative effects such as viscosity and heat conduction have not been included in the transport equations. Also in the hydrodynamical description of the plasma the equation associated with the law of conservation of baryon number has been dropped. However, three important problems have been considered here. Namely, the proper initialisation, the transverse motion of the plasma and the experimental signature of the plasma.

The effect of considering the full three-dimensional expansion of the plasma is that the local energy density falls off faster with respect to time than for the simple one-dimensional model. In our model, we find that ϵ is roughly proportional to $t^{-5/3}$ compare to $t^{-4/3}$ for the one-dimensional, scaling hydrodynamics. It was expected earlier[11,5] that the transverse expansion will not be significant until the late times i.e. roughly till 10fm/c. But the numerical simulation of initial conditions and the numerical solution of the hydrodynamic equations for the medium mass nuclei show that this assumption is not true. It is shown in chapter (3) of this thesis that the energy density fall off with respect to time is affected from the beginning of plasma expansion.

The most important conclusion of this thesis is that strangeness production can not serve as a signal for the plasma formation for medium mass nuclei. The number for the ratio of the strangeness to entropy obtained by using our model is of the order of 0.01, which corresponds to K^-/π^- ratio of the order of 0.054. Our estimate is lower by a factor of 4 than the recent estimates for K^-/π^- ratio for the same initial temperature. The number we have obtained is approximately the same as obtained for $p\bar{p}$ from the experiments[63]. Therefore, we find that for the quark-gluon plasma there is no K^-/π^- ratio enhancement over $p\bar{p}$ collisions. The reason why our model predicts such a small number for K/π ratio is as follows: the lifetime of the plasma predicted by simple models is much larger than the lifetime of the plasma predicted by the computer simulation. Therefore, there is not enough time for the strangeness production. Further, the high temperature region in the reaction is also more spatially limited, which also leads to less strangeness production.

For future studies, this model can be used for studying the other possible experimental signatures for the plasma formation such as the photon flux and dilepton production. There are a number of possibilities to improve this model, such as:

1. taking a more appropriate equation of state.
2. generating the initial conditions for different values of energy and the impact parameter.
3. calculating the production rate for the strange quarks more

precisely. One possibility is to calculate the one-particle distribution function at each time step and then use that in equation (4.11) to calculate the rates. This way the parametrization used for the reaction rate in equation (4.14) can be avoided and one can expect more accurate results.

4. doing the same simulation for heavy nuclei such as Pb or U. Another problem we did not look at is that what happens at and below the transition temperature: How does the quark-gluon plasma hadronizie? This is a very difficult question to answer without actually performing an experiment. Such experiments are being planned for the near future at CERN and at BNL.[12]

BIBLIOGRAPHY

1. Gell-Mann, M., Phys. Lett.8, 214 (1964)

2. Greenberg, O.W., Phys. Rev. Lett.13, 598 (1964)

3. Anishetty, R., Koehler, P. and McLerran, L., Phys. Rev. D22, 2783 (1980)

4. Bjorken, J.D., Phys. Rev. D27, 140 (1980)

5. Kajantie, K. and McLerran, L., Nucl. Phys. B214, 216 (1983)

6. Celik, J., Engels, J. and Satz, H., Phys. Lett. 129B, 323 (1983)

7. de Forcrand, Ph., Roiesnel, C., CERN preprint, TH.3858, Mar. 1984

8. Polonyi, J., Wyld, H.W., Kogut, J.B., Shigemitsu, J. and Sinclair, D.K., Phys. Rev. Lett. 53, 644 (1984)

9. Bjorken, J.D., Lecture Notes in Physics, Vol. 58, P.93, Springer, Berlin, 1976

10. Cleymans, J., Gavai, R.V. and Suhonen, E., Phys. Rep. 130, 217 (1986)

11. Bjorken, J.D., Phys. Rev. D27, 140 (1983)

12. Quark Matter '84, proceedings of the Fourth International Conference on Ultrarelativistic Nucleus-Nucleus Collisions, Helsinki, 1984, edited by K. Kajantie (Lecture Notes in Physics, Vol.221)(Springer, Berlin, 1985).

13. Busza, W. and Goldhaber, A.S., Phys. Lett. 139B, 235 (1984)

14. Date, S., Gyulassy, M. and Sumiyoski, H., Phys. Rev. D32, 619 (1985)

15. Landau, L., Izv. Akad. Nauk SSSR 17, 51 (1953)

16. Nix, J.R., Progr. Part. Nucl. Phys.2, 237 (1979)

17. Stocker, H., et al., Phys. Rev. Lett. 47, 1807 (1981)

18. Kapusta, J. and Strottman, D., Phys. Rev. C23, 1282 (1981)

19. Kapusta, J. and Strottman, D., Phys. Lett. 106B, 33 (1981)

20. Gavai, R.V. and Gocksch, Phys. Rev. D33, 614 (1986)

21. Chodos, A., Jaffe, R.L., Johnson, K., Thorn, C.B. and Weisskopf, V.F., Phys. Rev. D9, 3471 (1974)

22. Johnson, K., Acta Phys. Pol. B6, 865 (1975)

23. Hasenfratz, P. and Kuti, J., Phys. Rep. 40, 75 (1978)

24. Gyulassy, M., Kajantie, K., Kurki-Suonio, H. and McLerran, L., Berkeley preprint LBL-16277 (1983)

25. van Hove, L., Lecture at the Int. Conf. on Nuclear Physics, Florence, Italy 1983, preprint CERN TH.3725

26. Feinberg, E.L., Nuovo Cimento 34A, 391 (1976)

27. Domokos, G. and Goldman, J.I., Phys. Rev. D23, 203 (1981)

28. Kajantie, K. and Miettinen, H.I., Z.Physik C9, 341 (1981)

29. Rafelski, J., Phys. Rep. 88, 331 (1982)

30. Rafelski, J. and Muller, B., Phys. Rev. Lett. 48, 1066 (1982)

31. Rafelski, J., Nucl. Phys. A418, 215c (1984)

32. Kapusta, J. and Mekjian, A., Phys. Rev. D33, 1304 (1986)

33. Lifshitz, E.M. and Pitaevskii, L.P., "Statistical Physics 3rd edition", Pergamon Press,.Oxford (1980)

34. Bogolioubov, P.N., Ann. Inst. Henri Poincare 8, 163 (1967)

35. Celik, T., Engels, J. and Satz, H., Phys. Lett. 129B, 323 (1983).

36. Creutz, M., Jacobs, L. and Rebbi, C. Phys. Rep. 95. No. 4 (1983) 201-282.

37. Kajantie, K., Nucl. Phys. A418, 41c (1984)

38. Baym, G., Friman, B.L., Blaizot, J.P., Soyeur, M. and Czyz, W., Nucl. Phys. A407, 541 (1983)

39. Bjorken, J.D., Lectures given in Theoretical Particle Physics in Hamburg, Sept. 15-26, 1975, Proceedings Published as Current Induced Reactions, eds. J.G.Korner, G.Kramer and D.Schildknecht (Springer, 1976)

40. Alpgard, K. et al., Phys. Lett. 107B, 310 (1981)

41. Bialas, A., Czyz, W. and Lesniak, L., Phys. Rev. D25, 2328 (1982)

42. Elias, J.E. et al., Phys. Rev. D22, 13 (1980)

43. Weinberg, S., "Gravitation and Cosmology", J. Wiley and Sons, New York (1972)

44. Cooper, F., Frye, G. and Schonberg, E., Phys. Rev. D11, 192 (1975)

45. von Gersdoff, H., Mclerran, L., Kataja, M. and Ruuskanen, P.V., Phys. Rev. D34, 794 (1986)

46. Pratt, S., Phys. Rev. D33, 1314 (1986)

47. Kajantie, K., Raitio, R. and Ruuskanen, P.V., Nucl. Phys. B222, 152 (1983)

48. Chu, M.C., Phys. Rev. C31, 1739 (1985)

49. Boris, J.P. and Book, D.L., J. Comp. Phys. 20, 397 (1976)

50. Harlow, E.H., Amsden, A.A. and Nix, J.R., J. Comp. Phys. 20, 119 (1976)

51. Potter, D., "Computational Physics", J. Wiley and Sons, New York (1973)

52. Lapidus, L. and Pinder, G.F., "Numerical Solution of Partial Differential Equations in Science and Engineering", J. Wiley and Sons, New York (1982)

53. Abramowicz, H. et al., Z. Phys. C17, 283 (1983)

54. Gottschalk, T.D., Lectures at the 19th Int. School on Elementary Particle Physics, Kupari-Dubrovnik, Yougoslavia (1983); available as CERN Report TH.3810 (1984)

55. Cutler, R. and Sivers, D., Phys. Rev. D17, 196 (1978)

56. Altarelli, G. and Parisi, G., Nucl. Phys. B126, 298 (1977)

57. Payne, R.B., J. Fluid Mech. 2, 185 (1957)

58. Matsui, T., Svetitsky, B. and McLerran, L., Phys. Rev. D34, 783 (1986)

59. Georgi, H.M., Glashow, S.L., Machacek, H.E. and Nanopoulos, D.V., Ann. Phys. 114, 273 (1978)

60. Combridge, B.L., Nucl. Phys. B151, 429 (1979)

61. Landau, L., Proc. Acad. Sci. (USSR) Phys. Ser. 17, 51 (1953)

62. Hamilton, R.P., Pun, T.P., Tripp, R.D., Lazarus, D.M. and Nicholson, H., Phys. Rev. Lett. 44, 1182 (1980)

63. Alpgard, K. et al., Phys.Lett. 115B, 65 (1982)

64. Clare, R.B. and Strottman, D., Los Alamos National Laboratory preprint, LA-UR